UNIVERSITÉ DU QUÉBEC À MONTRÉAL

COMPARAISON DIRECTE DES SIMULATIONS CLIMATIQUES DE LA VERSION 5 DU MODÈLE RÉGIONAL CANADIEN DU CLIMAT (MRCC5) PAR RAPPORT AUX OBSERVATIONS BRUTES

MÉMOIRE
PRÉSENTÉ
COMME EXIGENGENCE PARTIELLE
DE LA MAÎTRISE EN SCIENCES DE L'ATMOSPHÈRE

PAR

RABAH HACHELAF

MARS 2016

REMERCIEMENTS

Je tiens à remercier mon directeur de recherche, le Professeur Pierre Gauthier, pour son soutien et sa disponibilité afin de réaliser cette étude. Je remercie également Ping Du, Katja Winger et Michel Valin pour leur support informatique et scientifique.

Mes remerciements vont également à tous les professeurs, étudiants et au personnel du Centre ESCER.

Finalement, je remercie ma femme Fella ainsi que les familles Hachelaf et Benbordi pour leur soutien moral au cours des années de cette maîtrise.

Ce projet a été financé par le programme de Subventions à la découverte du Conseil de Recherche en Sciences naturelles et génie (CRSNG) du Canada, le *Canadian Network for Regional Climate and Weather Processes* (CNRCWP) financé par le programme de Recherche sur les changements climatiques et sur l'atmosphère (RCCA) du CRSNG, par le Ministère du Développement Économique, de l'Innovation et de l'Exportation (MDEIE) du Québec et par Environnement Canada. La Faculté des sciences de l'UQAM m'a également accordé une bourse d'études. Je l'en remercie.

Ce travail a été rendu possible grâce aux ressources informatiques de Calcul Canada sur la plateforme Guillimin du consortium régional Calcul Québec.

TABLE DES MATIÈRES

LISTE DES FIGURES

LISTE DES TABLEAUX

LISTE DES ACRONYMES

3D-Var	Three-Dimensional Variational data assimilation
4D-Var	Four-Dimensional Variational data assimilation
AMSU	Advanced Microwave Sounding Unit
CanAM4	The Fourth Generation of the Canadian Atmospheric Global Climate Model
CanESM2	Second-Generation Canadian Earth system model
CORDEX	Coordinated Regional Climate Downscaling Experiment
CFSR	Climate Forecast System Reanalysis
CGCM	Coupled Global Climate Models
CMC	Canadian Meteorological Centre
CRCM5	Canadian Regional Climate Model, version 5
CRU	Climatic Research Unit
CONUS	Contiguous United States
ECHAM6	The Sixth Generation of European Centre/Hamburg Model
ECMWF	European Centre for Medium-Range Weather Forecasts
ERA-40	ECMWF Re-Analysis 40
ERA-Interim	ECMWF Re-Analysis Interim
FASTEM	Fast Ocean Surface Emissivity Model for Microwave frequencies
GEM	Global Environment Multiscale
GCM	Global Climate Model
HIRS	High-resolution Infrared Radiation Sounder
IASI	Infrared Atmospheric Sounding Interferometer
MCG	Modèle de Circulation Générale
MCGAO	Modèle de Circulation Générale Couplé Atmosphère-Océan

METAR	Meteorological Aerodrome Report
MGC	Modèle Global du Climat
MRC	Modèle Régional du Climat
MRCC5	Modèle Régional Canadien du Climat, Version 5
MPI-ESM-LR	Max Planck Institute for Meteorology's Earth System model Low Resolution version.
NCAR	National Center for Atmospheric Research
NCEP	National Centers for Environmental Prediction
NOAA	National Oceanic and Atmopsheric Administration
RCM	Regional Climate Model
RMSE	Root Mean Square Error
RTTOV	Radiative Transfert model for TIROS Operational Vertical sounder
SEVIRI	Spinning Enhanced Visible and InfraRed Imager
SHIP	Sea Surface Synoptic Observations
SYNOP	Surface Synoptic Observations
TEMP	Upper Air Soundings
Udel	University of Delaware
UTWV	Upper Troposphere Water Vapour

RÉSUMÉ

Dans cette étude, l'opérateur d'observation du système d'assimilation de données variationel tridimensionnel (3D-VAR) du Centre Météorologique Canadien (CMC) est utilisé afin d'évaluer la performance de différentes simulations climatiques sur l'Amérique du Nord et durant la période 2009-2013, issues de la 5^{e} Version du Modèle Régional Canadien du Climat (MRCC5) directement contre des observations brutes de différentes plateformes d'observations a savoir : les observations de surface, les radiosondages ainsi que les radiances satellitaires. L'opérateur d'observation est appliqué sur les simulations climatiques et permet de produire un équivalent de ces simulations au même temps et lieu où l'observation est faite, afin d'assurer la cohérence entre l'échantillon de données à valider et la référence.

Le but principal de cette étude est de présenter une façon différente de vérifier des simulations climatiques, et d'évaluer la cohérence de cette approche avec les méthodes de validation basées sur la comparaison contre des observations indirectes sur une grille ou des ré-analyses. En général, un bon degré d'accord a été noté entre les deux approches en termes de température, particulièrement sur la partie continentale des États-Unis, qui est caractérisée par un réseau homogène de stations météorologiques de surface. Par contre, un biais chaud systématique des températures à 2m d'environ +1 K a été observé en hiver, entre ERA-Interim et les observations sur le Canada et l'Arctique et conséquemment, la vérification des simulations climatiques contre ERA-Interim au-dessus de ces régions pourrait montrer un biais chaud excessif. Cependant, la température verticale des simulations CRCM5 pilotées par ERA-Interim se compare bien aux radiosondages, alors que les simulations pilotées par les Modèles de Circulation Générale Couplé Atmosphère-Océan (MCGAOs) présentent des grands biais, particulièrement au-dessus du niveau 300 hPa, pouvant être attribués en partie aux biais des MCGAOs ou à la variabilité climatique surtout dans la haute troposphère. Une bonne concordance a été remarquée entre ERA-Interim et les radiosondages pour toutes les saisons et sur toutes les régions de l'Amérique du Nord.

La vérification de l'humidité relative par rapport aux radiosondages n'a pas révélé de différences significatives des résultats pour les différentes simulations climatiques MRCC5 et ERA-Interim. On remarque toutefois qu'ERA-Interim a de la difficulté à reproduire le profil observé de l'humidité relative particulièrement aux niveaux moyens et supérieurs de l'atmosphère.

Les résultats de comparaison des équivalents-modèle de radiances produites à partir des simulations MRCC5 contre les radiances observées des canaux sensibles à la

température dans la haute troposphère ont montré une bonne concordance avec les comparaisons effectuées contre les radiosondages aux mêmes niveaux.

Les radiances satellitaires sensibles à la vapeur d'eau de la haute troposphère ont été utilisées pour examiner la performance des simulations MRCC5 à reproduire cette variable. En général, les simulations MRCC5 reproduisent mieux la vapeur d'eau dans la haute troposphère en hiver qu'en été par rapport aux observations satellitaires. Par contre, les biais significatifs observés dans les régions tropicales et subtropicales peuvent être attribués à la capacité du modèle à représenter adéquatement la vapeur d'eau dans l'atmosphère et à la convection qui la transporte vers les niveaux supérieurs de l'atmosphère.

Finalement, les observations satellitaires peuvent être une référence pertinente pour évaluer les différentes composantes des modèles climatiques, grâce à leur distribution spatiale qui couvre des régions inaccessibles ou pauvres en termes de disponibilité d'observations conventionnelles.

MOTS-CLÉS: Assimilation de données, opérateur d'observation, observations météorologiques, radiances satellitaires, validation, modèle régional du climat.

CHAPITRE I

INTRODUCTION

Les études sur le climat et les changements climatiques ont connu un grand essor grâce aux Modèles de Circulation Générale (MCGs) connu aussi sous le nom Modèles Globaux du Climat (MGCs). Ces modèles mathématiques très complexes cherchent à reproduire les conditions climatiques passées, présentes et futures sur tout le globe à une résolution horizontale d'une centaine de kilomètres. Afin d'étudier les processus atmosphériques qui se produisent à des échelles spatiales plus fines, les climatologues ont eu recours aux Modèles Régionaux du Climat (MRCs), ces derniers ont permis de simuler les variables climatiques à des résolutions horizontales de l'ordre de dizaines de kilomètres. Les MRCs ont besoin de conditions aux frontières pour modéliser le climat sur une région déterminée. Ces conditions sont fournies par des Modèles de circulation générale couplés atmosphère-océan (MCGAO) ou par des ré-analyses météorologiques.

Les simulations climatiques issues des MRCs produisent des représentations de l'état de l'atmosphère sur une région qui doivent être évaluées afin de connaître leur capacité à reproduire le climat présent et ensuite le climat futur. La capacité d'un MRC à reproduire le climat passé est garante de sa capacité à simuler le climat futur avec fiabilité.

La plupart des méthodes d'évaluation des MRCs sont basées sur la comparaison des simulations climatiques par rapport à des ré-analyses météorologiques comme par exemple celles produites par le Centre Européen de Prévision Météorologique à

Moyen Terme (CEPMMT mieux connu par son acronyme anglais, ECMWF) Re-Analysis 40 (ERA-40) (Uppala *et al.*, 2005), ERA-Interim (Dee *et al.*, 2011) et celles du National Center for Environmental Prediction/National Center for Atmospheric Research (NCEP/NCAR) (Kalnay *et al.*, 1996). La validation de ces simulations est également faite à travers une comparaison à des données d'observations météorologiques prétraitées et interpolées sur une grille régulière (gridded observation data) comme celles produites à l'Université du Delaware (Udel, Willmott and Matsuura, 1995) ou encore celles produites par le Climate Research Unit (CRU, Mitchell and Jones, 2005).

Ces données de référence sont produites avec différentes méthodes statistiques et algorithmes mathématiques. L'assimilation de données variationnelle tri- ou quadri-dimensionnelle (3D/4D-VAR) (Courtier *et al.*, 1997 ; Rabier *et al.*, 2000) sont utilisées pour produire les ERA-40 et ERA-Interim respectivement. L'assimilation de données est basée sur une combinaison d'un état de l'atmosphère estimé *a priori* par un modèle numérique de prévision du temps avec plusieurs types d'observations météorologiques conventionnelles (e.g., les observations des stations de surface, des bateaux, des bouées, des radiosondages) et non-conventionnelles (les radiances satellitaires, les radio-occultations GPS, les observations des avions commerciaux,...etc) afin d'obtenir le meilleur estimé de l'état de l'atmosphère dans le passé, appelé *ré-analyse*. La base de données de référence CRU a été créée à partir d'une interpolation horizontale des anomalies des observations des stations calculées par rapport à une période de référence de 1961-90 durant laquelle l'homogénéité des observations a été vérifiée (Mitchell and Jones, 2005. Harris *et al.* 2013). Les données Udel sont construites en utilisant une procédure d'interpolation dite "intelligente" des moyennes des observations mensuelles sur une grille de 0.5° pour la période 1901-2010. Cette procédure intègre un modèle numérique d'élévation (Digital-Elevation Model DEM, interpolation assistée) pour tenir compte des effets de la topographie sur la température à 2m et les précipitations (Willmott and Matsuura, 1995 ; Willmott and Robeson, 1995).

De grandes variations dans la couverture, la nature et la qualité des observations dans les différentes régions affectent directement les ré-analyses. À titre d'exemple, les stations météorologiques de surface et les radiosondages ont une meilleure couverture et distribution sur l'hémisphère nord par rapport à l'hémisphère sud ou les océans (sauf pour quelques stations isolées sur des îles).

Par contre, ces données d'observations sur grille ou ces ré-analyses ne sont pas toujours précises dû à l'imperfection des différentes méthodes et techniques employées pour créer de l'information sur une grille régulière à partir du réseau d'observations éparses. Martynov *et al.* (2013) ont constaté d'importantes différences entre les données ERA-Interim, Udel et CRU TS 2.10 sur l'Amérique du Nord pour la température à 2 m. Mearns *et al.* (2012) ont noté aussi des différences entre Udel et CRU TS 2.10 sur la partie continentale des Etats-Unis, particulièrement sur la côte ouest dû à la présence des Rocheuses. De telles différences dans ces données dites de "référence" peuvent influencer significativement les résultats et les conclusions sur la performance des MGGs et MRCs.

CRU et Udel sont des données de référence largement utilisées dans la communauté scientifique. Par contre, elles constituent des moyennes mensuelles ne permettant pas d'étudier les cycles diurnes ou la variabilité intra-mensuelle. De plus, elles ne sont disponibles que sur les continents.

En comparant les simulations de plusieurs MRCs avec des observations sur une grille régulière ou des ré-analyses à différentes résolutions horizontales, il est nécessaire de prendre en considération la différence de résolution entre eux. Il n'est pas recommandé de faire une interpolation arbitraire d'une grille vers une autre pour calculer les différences, la comparaison doit être effectuée sur la grille ayant la résolution la plus grossière entre les différentes simulations et observations sur une grille. Il est souhaitable aussi d'utiliser des moyennes spatiales au lieu d'une interpolation bilinéaire pour passer d'une grille à fine résolution vers une autre à une résolution grossière. (Hong and Kanamitsu, 2014).

Des études antérieures faisant des comparaisons directes des ré-analyses contre des observations de surface et des radiosondages, ont démontré que les ré-analyses ne sont pas toujours en accord avec les observations. Mooney *et al.* (2010) ont comparé les données des stations météorologiques en Irlande avec les ré-analyses ERA-40, ERA-Interim et NCEP/NCAR durant la période 1989-2001. Ils ont conclu que les trois ré-analyses surestiment la température à 2m en hiver à cause du traitement différent des températures à la surface sur terre et sur mer. Bao *et al.* (2012) ont évalué ces trois mêmes ré-analyses par rapport à des radiosondages indépendants qui ne sont pas assimilés dans la production de ces ré-analyses pendant les trois mois de la campagne Tibetan Plateau Experiment (TIPEX-1998). Ils ont montré que les ré-analyses présentent des biais relativement faibles pour la température et la vitesse du vent, mais des biais considérables pour l'humidité relative. Sur l'Océan Arctique Central, Jakobson *et al.* (2012) ont évalué plusieurs ré-analyses par rapport à des radiosondages indépendants et ils ont constaté que les profils verticaux des ré-analyses présentent des erreurs significatives pour la température et l'humidité relative sur cette région.

Au cours des dernières années, un progrès considérable a été fait dans l'utilisation de la télédétection par satellite pour la surveillance du climat afin d'améliorer la compréhension du système climatique et des effets du réchauffement anthropique. Certaines découvertes importantes impliquant l'interaction entre les aérosols, l'atmosphère et les océans, ne pouvaient pas être trouvées sans l'apport des observations satellitaires, par exemple, l'élévation du niveau de la mer à cause de la fonte des glaciers et l'effet de refroidissement en surface à cause de l'augmentation de la concentration des aérosols dans la stratosphère. D'autres découvertes sont documentées par Yang *et al.* (2013).

La vapeur d'eau dans la haute troposphère est parmi les composantes importantes du système climatique. Elle est le principal gaz à effet de serre dans la troposphère et sa variabilité influence directement le bilan radiatif de la Terre. Sa distribution spatiale

est étroitement liée à la circulation générale de l'atmosphère, à la convection et à d'autres composantes du cycle hydrologique (Iacone *et al.*, 2003).

Plusieurs études ont utilisé les observations satellitaire pour évaluer la capacité des MRCs à reproduire le patron observé de la vapeur d'eau dans la haute troposphère et pour étudier son influence sur les autres composantes du climat.

Allan *et al.* (2003) ont comparé l'humidité simulée par le modèle de climat du Centre Hadley par rapport aux radiances satellitaires provenant de sondeurs dans l'infrarouge à haute résolution HIRS (High Resolution Infrared Sounder), sensible à la vapeur d'eau. Ils ont constaté que la distribution et la variabilité des données satellitaires sont raisonnablement bien simulées par le modèle sur les régions tropicales. Par contre, le modèle surestime les observations satellitaires dans les régions subtropicales.

Iacone *et al.* (2002) ont réalisé une étude pour valider un nouveau modèle radiatif pour les ondes longues du modèle de climat communautaire du NCAR en utilisant les radiances satellitaires de l'instrument HIRS. Ils ont aussi montré la possibilité de capturer les signatures des épisodes de la mousson et d'El Niño en termes de contenu en vapeur d'eau dans la haute troposphère détectée par les observations satellites.

Notre étude propose l'utilisation des observations brutes des stations de surface, de radiosondages et des observations satellitaires comme données de référence pour évaluer différentes simulations climatiques de la version 5 du Modèle Régional Canadien de Climat (MRCC5). L'objectif est de comparer directement les simulations climatiques aux observations, à la position et au temps correspondant.

Le principal avantage d'une comparaison directe contre des observations est d'éviter les erreurs causées par les incertitudes liées aux méthodes utilisées pour produire les observations sur une grille telles que celle de CRU et de Udel, ainsi que les ré-analyses qui incluent de l'information issue du modèle utilisé dans le processus d'assimilation de données. De plus, les observations brutes constituent une référence indépendante pour évaluer n'importe quelle simulation climatique pilotée par des ré-analyses ou par des MCGs, parce que l'évaluation d'un RCM ne peut être considérée

comme complètement indépendante de la référence si elle est faite par rapport à la même ré-analyse qui est utilisée pour le pilotage de la simulation.

Dans notre étude, nous allons aussi comparer les ré-analyses ERA-Interim aux observations brutes afin d'évaluer leur précision et leur cohérence spatiale et temporelle sur différentes régions de l'Amérique du Nord. Les radiances satellitaires sont aussi utilisées pour profiter de leur couverture spatiale sur les régions inaccessibles ou pauvres en observations, afin d'évaluer la température et le contenu en vapeur d'eau dans la haute troposphère des différentes simulations du MRCC5.

Organisation du mémoire

Suite à cette introduction, un article en préparation rédigé en anglais est présenté au chapitre II et constitue le corps de ce mémoire. Cet article comprend tout d'abord une introduction à la section 2.1, dans laquelle une revue de la littérature et le contexte scientifique du sujet de cette étude sont présentés. La méthodologie est présentée à la section 2.2, et décrit l'utilisation de l'opérateur d'observation d'un système d'assimilation de données qui effectue le passage de l'espace modèle vers l'espace des observations pour permettre la comparaison directe entre une simulation climatique et des observations brutes. Les observations et les simulations climatiques utilisées dans notre étude sont décrites aux sections 2.3 et 2.4 respectivement.

Les résultats seront présentés dans trois sections suivant le type des observations : les observations de surface (Section 2.5), les radiosondages (Section 2.6) et les radiances satellitaires (Section 2.7). Finalement, le résumé et les conclusions de cet article seront formulés dans la Section 2.8. Le mémoire se termine par une présentation des conclusions en français au chapitre III et des références.

CHAPITRE II

COMPARAISON DIRECTE DES SIMULATIONS CLIMATIQUES DE LA VERSION 5 DU MODÈLE RÉGIONAL CANADIEN DU CLIMAT (MRCC5) PAR RAPPORT AUX OBSERVATIONS BRUTES

Ce chapitre est présenté sous forme d'un article scientifique rédigé en anglais. Les parties *Introduction* et *Methodology* traitent les motivations et l'approche suivie dans la réalisation de cette étude. Les parties *Characteristics of the observations* et *Description of the climate simulations* décrivent les différents types d'observations et de simulations climatiques impliqués. Les résultats des différentes expériences sont présentés suivant le type d'observation dans les sections suivantes: *Comparison with surface temperature observations*, *Comparison with radiosondes observations* et *Comparison with satellite observations*. La dernière partie *Summary and conclusion* est un résumé des expériences menées et des principaux points retenus de cette étude.

Direct comparison of climate simulations from Canadian Regional Climate Model, Version 5 (CRCM5) against raw observations

by

Rabah Hachelaf [1] and Pierre Gauthier

ESCER Centre, *Department of Earth and Atmospheric Sciences*
Université du Québec à Montréal (UQAM), Montréal (Québec), Canada

[1] Corresponding author: Rabah Hachelaf, ESCER Centre
Department of Earth and Atmospheric Science
Université du Québec à Montréal
P.O. Box 8888 Downtown Station
Montréal (Québec)
CANADA H3C 3P8
Email: hachelaf@sca.uqam.ca

Abstract

The observation operator of a three-dimensional variational data assimilation system (3D-VAR) was used to evaluate the performance of different climate simulations produced with the Canadian Regional Climate Model, version 5 (CRCM5) driven by ERA-Interim reanalysis (ERA-INT) or two Coupled Global Climate Models (CGCMs) over North America for the 2009-2013 period. This permits a direct comparison against raw observations provided by weather surface stations, radiosondes and satellite instruments. The observation operator produces a climate simulation equivalent of those observations at their exact location and time. The main objective of this study is to present different ways to assess the consistency of the verification of climate simulations based on this approach and those based on a comparison with gridded-observation data sets or reanalyses. In general a good agreement has been noted, particularly over Contiguous United States (CONUS) which is characterized by a homogeneous network of weather stations. However a systematic near surface temperature warm bias has been noted between ERA-INT and observations over Canada and the Arctic, so that a verification of a climate simulation with respect to ERA-interim in these regions would wrongly be interpreted as a bias. While upper-air temperature from CRCM5 simulations driven by ERA-INT agrees well with radiosonde observations, simulations driven by CGCMs present large biases particularly at levels above 300hPa, due in part to climate variability or to the CGCMs own biases.

Verification of relative humidity against radiosonde observations reveals no significant differences between the different CRCM5 simulations. However, ERA-INT has difficulty to reproduce the observed relative humidity especially at mid and higher levels. Comparing against satellite radiance data which provide a better spatial horizontal coverage, results agree with those of the comparison of CRCM5 simulations against radiosondes observations. Satellite radiances are sensitive to upper tropospheric water vapour (UTWV) and are used to examine the UTWV from CRCM5 simulations which perform better in winter than in summer at reproducing UTWV pattern. Large differences with respect to the satellite data are noticed over subtropical regions, which could be attributed to a model weakness in representing water vapour within lower levels and its horizontal and vertical transport to mid and upper levels.

Keywords: Data Assimilation - Observation Operator - Raw observations, Satellite Radiances – Validation - Canadian Regional Climate Model.

2.1 Introduction

Simulations from regional climate models (RCMs) must be assessed to evaluate their capability to reproduce present climate parameters at small scales. Most RCMs assessments compare simulated climate fields against reanalyses such as the European Centre for Medium-Range Weather Forecasts Re-Analysis-40 ERA-40 (Uppala *et al.*, 2005), ERA-Interim (Dee *et al.*, 2011) and the National Centers for Environmental Prediction/National Center for Atmospheric Research (NCEP/NCAR) reanalysis (Kalnay *et al.*, 1996) or gridded observation data sets like that of the University of Delaware (Udel, Willmott and Matsuura 1995) and the Climate Research Unit (CRU, Mitchell and Jones 2005).

Those reference datasets can be produced by different methods. The data assimilation systems such as four-dimensional variational data assimilation system (4D-VAR) was used in the case of ERA-Interim, which combine an *a priori* atmospheric estimate obtained from a numerical weather prediction model with several types of observations to construct the best past atmospheric state estimate, an analysis (Rabier *et al.*, 2000). A different method is used to produce CRU TS3.10 data. First the inhomogeneities of station observations over a normal climate reference period from 1961-90 is checked, then station anomalies are interpolated to a 0.5° grid covering land (excluding Antarctica) to produce monthly climate gridded data for the period 1901-2013 (Mitchell and Jones, 2005). The Udel data from 1901-2010 are constructed by using a "smart" interpolation procedure of monthly station observations at a 0.5° resolution grid including a digital-elevation-model (DEM), which corrects the 2-m temperature and precipitations before being interpolated (Willmott and Matsuura, 1995; Willmott and Robeson, 1995).

However, these datasets are not perfectly accurate. First, the large variation in the accuracy and the coverage, nature and quality of observations in different regions affect directly the analyzed fields. For example, the radiosonde network and aircraft measurements ensure a better coverage over the Northern hemisphere than over the

Southern hemisphere or oceans. Secondly, different methods must be used to create a derived observation values field from a scattered observation network over a regular grid which leads to significant differences due to the different approaches that were employed. Martynov *et al.* (2013) found important differences between ERA-Interim, CRU TS 3.1 and Udel observation gridded datasets over North America in terms of 2m surface temperature. Mearns *et al.* (2012) noticed some differences between Udel and CRU TS 2.10 datasets for the contiguous United States (CONUS) domain particularly over complex terrain regions. Such differences in "reference" datasets could impact significantly the conclusions drawn about the bias (or performance) of a given climate simulation. Thirdly, even though the CRU TS3.1 and Udel are amongst the most used observation datasets by the climate community, they only provide monthly surface means and do not consider data available over oceans which cover almost 71% of the Earth's surface. Finally, when comparing the skills of RCMs simulations using gridded observations or reanalyses, it is necessary to take into account the horizontal resolution. Interpolation form coarse to fine resolution domains may not be appropriate and the interpolation must be performed by taking spatial scales into consideration (Hong and Kanamitsu, 2014).

Our study proposes to use raw ground-based and satellite observations as reference data to assess different simulations provided by the fifth-generation Canadian Regional Climate Model (CRCM5). The objective is to compare the simulated climate directly against observations at the time and location where the observation was made. The main advantage of this approach is to avoid errors caused by uncertainties due to the method used to produce observation-based reference (like CRU TS3.10 and Udel) and reanalyses which also embed information provided by the model used in the assimilation process. Moreover, raw observations constitute an independent reference to assess any simulation driven by reanalyses or by Coupled Global Climate Models (CGCMs), since the evaluation of regional climate simulations cannot be considered completely independent from the reference if the

assessment is made by the same reanalysis used to drive the RCM (Separovic *et al.*, 2013).

Previous studies used a direct comparison of reanalyses against surface and upper air observations which revealed that reanalyses do not always fit observations. Mooney *et al.* (2010) compared 2m surface temperature data at stations over Ireland for the period 1989-2001 against ERA-40, ERA-Interim and NCEP/NCAR reanalyses and found that the three reanalyses overestimate the 2m surface temperature in winter. Bao *et al.* (2012) evaluated NCEP-CFSR, NCEP-NCAR, ERA-Interim and ERA-40 reanalyses with respect to independent radiosondes for a period of three months during the Tibetan Plateau Experiment (TIPEX, 1998). They showed that each reanalysis presents a relatively small mean bias for temperature and horizontal wind speed but a considerable bias in the mean relative humidity. Over the central Arctic Ocean, Jakobson et *al.*, (2012) compared several reanalyses against independent radiosondes (not assimilated by the models) and found that all reanalyses suffered from large errors in the vertical profiles of temperature and relative humidity.

In the present study, satellite observations have also been used to evaluate the performance of some components of the CRCM5 simulations. In recent years considerable progress has been made in understanding the climate system and its interaction with the anthropogenic warming by using satellite remote sensing for climate monitoring. Some important discoveries about the climate system and its interaction with the oceans and the stratosphere have been highlighted by Yang *et al.* (2013), which could not have been found without satellite observations, in particular, the rising of sea-level and the cooling effects of increased stratospheric aerosols.

Upper troposphere water vapour is an important component of the climate system since it is the primary greenhouse gas in the troposphere and its variability impacts directly the Earth's radiation budget. Its distribution is closely related to the dynamics of the atmospheric general circulation, the occurrence of convection and other components of the hydrological cycle (Iacone *et al.*, 2003). Many studies have

evaluated the ability of RCMs at reproducing the observed pattern of upper troposphere water vapour by satellite observations and study its feedback in climate models (Paltridge *et al.*, 2009). Allan *et al.* (2003) compared the moisture in the Hadley Centre climate model with respect to High Resolution Infrared Sounder (HIRS) satellite radiances. Iacone *et al.* (2002) did a similar study for the NCAR community Climate model and evaluated the impact of a new longwave radiation model; they were also able to detect the signature of Monsoons and El-Nino episodes in term of upper tropospheric moisture using satellite observations.

The present article is organized as follows. Section 2.2 presents the methodology used to transform CRCM5 simulations from model to observed space using the observation operator. Section 2.3 presents the experimental framework and the characteristics of the different type of observation and climate simulations used. Sections 2.4, 2.5 and 2.6 present comparisons of climate simulations with respect to surface, upper-air and satellite observations respectively to estimate biases and Root Mean Square Errors (RMSE). Finally a summary and conclusions are presented in section 2.7.

2.2 Methodology

Data assimilation methods consist in estimating the best possible atmospheric state, using a combination of a forecasted atmospheric state with a large range of observations including surface and upper air observations and also non-conventional observations like satellite radiances and aircrafts measurements. In this study, to be able to comparing climate simulations against scattered observations, the observation operators from the Canadian Meteorological Center (CMC) three-dimensional variational (3D-VAR) assimilation system is employed (Gauthier *et al.*, 1999, 2007; Buehner *et al.*, 2015).

A general formulation of a variational data assimilation scheme can be summarized as a statistical estimation principle in which an analysis $\mathbf{X}_a$ is represented as a corrected of a background state $\mathbf{X}_b$ based on the departure between the model equivalent of observations **y**. This translates as

$$\mathbf{X}_a = \mathbf{X}_b + \mathbf{K}\left(\mathbf{y} - \mathbf{H}(\mathbf{X}_b)\right) \qquad (1)$$

where $\mathbf{X}_a$ is the optimal analysis field, $\mathbf{X}_b$, the model background state usually a short-range forecast in numerical weather prediction, which is made from 3D gridded-fields for all prognostic model variables, namely the horizontal wind components, temperature, specific humidity, surface pressure and ground temperature. The nonlinear observation operator, **H**, links a model state to the observations represented here by the vector **y**, the observation vector while **K** is the optimal gain matrix defined to minimize the analysis error variance. Information about the accuracy of the background state and the observations are expressed through their background and observation error covariances, **B** and **R** which enables to write the gain matrix as $\mathbf{K} = \mathbf{B}\mathbf{H}^T\left(\mathbf{R} + \mathbf{H}\mathbf{B}\mathbf{H}^T\right)^{-1}$.

The innovation $\mathbf{d} = \mathbf{y} - \mathbf{H}(\mathbf{X}_b)$ represents the difference between the observation value and the model equivalent of the observation and needs to be evaluated for all observations at each analysis time. The observation operator **H** contains all operations needed to go from gridded model variables to observations' equivalent. It includes horizontal and vertical interpolation operators to obtain a model equivalent of the observations at their location using a horizontal bilinear interpolation based on the four grid points surrounding the observation location. Moreover, for a comparison to satellite radiances, **H** includes also a fast radiative transfer model to compute model brightness temperatures that can be compared directly against observed radiances from satellites. The CMC variational assimilation system uses the Radiative Transfert

model for TIROS Operational Vertical Sounder (RTTOV), Version 8.7 (Saunders *et al.*, 1999).

To calculate the simulated radiance L^{Clr} in clear sky conditions, RTTOV requires temperature, specific humidity profiles, surface skin temperature and surface pressure. Ozone profiles and surface emissivity over continent are taken from a monthly climatology data base. Surface emissivity over ocean is calculated regarding the sea state from surface wind speed using the Fast Microwave Ocean Surface Emissivity model for Microwave frequencies (FASTEM-3) (English *et al.*, 2003).

The simulated top of upwelling radiance in clear sky, $\boldsymbol{L^{Clr}}$, at a frequency $\boldsymbol{\nu}$ and viewing angle $\boldsymbol{\theta}$ can be written as

$$L^{Clr}(\nu,\theta) = \tau_s(\nu,\theta)\varepsilon_s(\nu,\theta)B(\nu,T_s) + \int_{\tau_s}^{1} B(\nu,T_s)d\tau + \left(1-\varepsilon_s(\nu,\theta)\right)\tau_s^2(\nu,\theta)\int_{\tau_s}^{1}\frac{B(\nu,T)}{\tau^2}d\tau \quad (2)$$

Where τ_s the surface to space transmittance ε_s is the surface emissivity, $B(\nu,\tau)$ the Planck function for a frequency ν and temperature T, the transmittance τ at each vertical level and T_s the surface temperature. Equation (2) shows that simulated radiances are affected by two principal contributions: the first one is from the surface, represented by the first and the third term (emitted and reflected assuming specular reflexion) while the second is the atmosphere contribution. RTTOV could simulate several types of satellite radiances from different sensors such as: AMSU, HIRS, SEVIRI, IASI and others.

The observation vector **y** contains different types of observations from conventional ground-based observations like temperature, winds and pressures from surface stations, radiosondes or aircraft, but also remotely sensed measurements such as satellite radiances. In the framework of numerical weather prediction, the assimilation system permits to correct a short-term model forecast through a comparison to all

those observations. Using statistical estimation principles, this produces the analysis which is the best estimate of the atmospheric state.

In our study, the background state was replaced by climate simulation. Hence, if $\mathbf{x}_c(t)$ stands for the state of the climate model simulation at time *t*, the innovation from observations is then:

$$\mathbf{d}(t) = \left(\mathbf{y} - \mathbf{H}(\mathbf{x}_c(t))\right) \approx \boldsymbol{\varepsilon}_o - \mathbf{H}\boldsymbol{\varepsilon}_c, \tag{3}$$

Where **y** stands for the observations valid at that time while $\boldsymbol{\varepsilon}_o$, is the observation error and $\mathbf{H}\boldsymbol{\varepsilon}_c$ is the error of the simulation expressed in terms of the observed quantities. Here, **H'** represents the linearization (Jacobian) of the observation operator evaluated with respect to $\mathbf{x}_c$ taken at the time and location of the observation. The average of **d**(t) is then :

$$\overline{\mathbf{d}(t)} \approx \overline{\boldsymbol{\varepsilon}_o - \mathbf{H}'\boldsymbol{\varepsilon}_c} = \overline{\boldsymbol{\varepsilon}_o} - \overline{\mathbf{H}'\boldsymbol{\varepsilon}_c} \tag{4}$$

Where $\overline{(\cdots)}$ stands for such spatial and time averaging made over all observations available during a period of time and within a particular region. It is important to stress that this diagnostic includes biases from both the observations and the model itself. If observations are assumed to be unbiased, then this reveals the observable bias of the model.

Bias and Root Mean Square Error (RMSE) (Jolliffe and Stephenson, 2012) are used as metrics to evaluate the performance of CRCM5 climate simulations using raw observations. Due to the irregularity of observations, averages are performed over North America and three sub-regions: Contiguous United States (CONUS), Canada and Arctic (represented in Fig. 2.6). Averaging is also done over time periods like winter and summer seasons. Averaged Bias and RMSE during winter and summer seasons and over a particular region will be given as:

$$Bias = -\overline{\mathbf{d}(t)} \text{ , and} \qquad RMSE = \overline{\sqrt{\frac{\sum_{i=1}^{n} \| \mathbf{d}_i(t) \|^2}{n}}} \text{ , } \qquad (5)$$

A grid-to-grid comparison of climate simulations with respect to ERA-Interim will also be performed over the same domains and periods to evaluate possible differences between the two approaches and to examine the level of agreement between validation using reanalysis and raw observations.

It is important to keep in mind that no data assimilation process has been done in this study, only the observation operator is applied to climate simulations and ERA-Interim to get the observation departures from climate simulations out of which bias and RMSE can be obtained. This will permit to compare in a consistent manner the different climate simulations against conventional and satellites observations. A direct comparison to observations is limited by the available observations. However, we need to keep in mind that any reanalysis is a combination of a short-term forecast with observations, so in areas of data voids, the analyzed values in those areas reveal mostly the model forecast that was used as a background state.

2.3 Characteristics of the observations

The observations used are those assimilated within the CMC data assimilation system over North America. The objective is to compare different CRCM5 simulations against those verified observations with a particular emphasis on essential climate variables at the surface and in the troposphere. These include near surface temperature, temperature and relative humidity profiles, upper tropospheric temperature and water vapor. This will be performed over a period of five years from 2009 to 2013 for the winter and summer seasons.

The motivation for using those data is to be sure that those reference datasets are not affected by any errors generated by the method, model or the assimilation technique used to produce gridded observation data sets or reanalysis. The surface observation network over North America, shown in Fig. 2.2a, has a regular and dense distribution of weather stations over the continent especially between 20°N and 60°N latitude. Over Canada, the distribution is concentrated near the US-Canada borders with a particularly dense network in the South of Alberta. As will be seen later, having a uniform distribution of observations benefits the estimate of the bias and RMSE.

Upper air data from radiosondes were used as a reference to examine the vertical structure of climate simulations. About 150 soundings are available over North America (Fig. 2.2b) at 00 and 12 UTC, which represent about 26% of all soundings launched globally. As shown in Fig. 2.2b, most radiosondes are over CONUS and are regularly distributed, giving a good coverage and representativity of meteorological variables over the troposphere. Over Canada and Arctic regions the radiosondes network may not be dense enough to represent and capture all atmospheric processes occurring over those regions.

Observations from satellites will also be used to evaluate the climate simulations; those are used in data assimilation to produce reanalyses (Dee and Uppala, 2009). They offer a global coverage and are particularly useful over oceans and remote regions where conventional meteorological observations are sparse or nonexistent. Several studies used satellite observations to retrieve or diagnose surface parameters like ice over and sea surface temperature (Hall *et al.*, 2012), or upper-air parameters like water vapour and clouds (Jiang *et al.*, 2012).

In our study, satellite observation from the Advanced Microwave Sounding Unit (AMSU) are used, AMSU is a cross-scanning passive microwave sounding instrument onboard the polar operational meteorological satellites NOAA-15, 16 and 18. The scan patterns and geometric resolution translate to a 48 km resolution at nadir with a 2074 km swath width from the 837 km nominal orbital altitude. Fig. 2.3 shows

a distribution example of AMSU radiances over a ±3 h time window centered at 00 UTC, which could be slightly different from a time window to another. There are two types of AMSU instruments. AMSU-A is a multi-channel microwave radiometer which measures radiances in 15 discrete frequency channels (23-90 GHz). Channels 3 to 14 are sensible to the thermal radiation in the 50-60 GHz oxygen band at various atmospheric layers described by the weighting functions displayed in Fig. 2.4 (Kidder *et al.*, 2000). AMSU-B has the same technical characteristics as AMSU-A except, that it has five channels numbered 16 to 20 of overall AMSU instrument but referred to as AMSU-B Channels 1 to 5. The AMSU-B Channel 3, 4 and 5 are at frequencies near a strong water vapour spectral line at 183.31 GHz (Saunders *et al.*, 1995). These channels are used to diagnose upper tropospheric water vapour and retrieve moisture profiles (Rosenkranz, 2001).

AMSU-B Channel 3 has been used here to assess the water vapour in the upper troposphere. As shown in Fig. 2.5 from Deeter and Vivekanandan (2005), the weighting function of this channel peaks at an altitude near 6 km and is not affected by the surface. The satellite radiances from this channel are then suitable to evaluate the water vapour content in the upper troposphere.

The observations used in our study are:

- 2m surface temperature from airport weather stations (METARs), synoptic weather stations (SYNOPs) and from marine stations (SHIPs) available every 6 hours,
- Vertical temperature and relative humidity profiles from radiosondes interpolated to the analysis pressure levels available every 12 hours.
- Satellite radiances converted into brightness temperatures from AMSU-A Ch7, Ch8 and AMSU-b Ch3 available over a ±3 hours time window at every 6 hours.

All observation datasets, and particularly satellite radiances, have been quality controlled through the CMC operational assimilation system to identify and remove erroneous data. Satellite radiances have benefited from a bias correction to remove systematic errors associated with the instruments (Gauthier *et al.,* 2003; Chouinard and Hallé, 2003). Table 2.1 summarizes all observations that will be used in our experiments.

2.4 Description of the climate simulations used

The fifth-generation of the Canadian Regional Climate Model, (CRCM5) (Zadra *et al.*, 2008) is based on a limited-area version of the Global Environment Multiscale (GEM) model used for Numerical Weather Prediction at Environment Canada (Côté *et al.*, 1998). Here, the CRCM5 is used over the North American COrdinated Regional climate Downscaling EXperiment (CORDEX) domain (Fig. 2.1). Details about the discretization, dynamic, physics and land surface schemes used by the CRCM5 can be found in Martynov *et al.* (2013) and Hernandez-Diaz *et al.* (2012).

Four different CRCM5 simulations from 2009 to 2013 have been used, taken from previously spun up simulations involved in the North American CORDEX. Two sets of simulations are driven by ERA-Interim lateral and surface boundary conditions at a horizontal resolution of 0.44° and 0.22°. The boundary conditions are specified on pressure levels for temperature, horizontal wind components and specific humidity and at the surface, the mean sea level pressure, sea surface temperature (SST) and sea ice fraction were used. Two other simulations with a resolution of 0.44° were forced laterally by two Coupled Global Climate Models (CGCMs). The first is the Second-Generation Canadian Earth system model (CanESM2) (Arora *et al.*, 2009, 2010) and the second is the Max Planck Institute for Meteorology's Earth System model in its Low Resolution version (MPI-ESM-LR) (Roeckner *et al.*, 2003; Giorgetta *et al.*,

2012). Details about these two climate simulations and driven variables can be found in Separovic *et al.* (2013). The full resolution ERA-Interim reanalysis at a horizontal resolution of 0.75° and 60 model levels (available online at: http://data-portal.ecmwf.int) up to 0.01 hPa is also used as a reference climate simulation to evaluate the analyzed and the observed climate in observation space. All CRCM5 simulations and ERA-Interim reanalysis are post-processed on 80 hybrid levels with the top level near 0.1 hPa to be consistent with the observation operator described in Section 2.2.

Using those different climate simulations and a reanalysis allows us to compare the simulated and analyzed climates over North America versus the observed climate estimated from different raw observations and then evaluate the impact of lateral and surface boundaries driving data and the increase of the horizontal resolution on the simulation from these different perspectives.

In what follows, the acronyms CRCM-ERA, CRCM-CAN and CRCM-MPI will designate CRCM5 simulations at a resolution of 0.44° driven by ERA-Interim reanalyses, CanESM2 and MPI-ESM-LR, respectively. Similarly, CRCM0.22-ERA is same as CRCM-ERA but at a horizontal resolution of 0.22°. Finally, the ERA-INT experiment is a comparison of ERA-Interim against the same set of observations as the other experiments. A summary of the assessed climate simulations presented in this study is shown in Table 2.2.

2.5 Comparison with surface temperature observations

In this section, a comparison of 2m surface temperature from different CRCM5 simulations is made with respect to surface observations from METARs, SYNOPs and SHIPs. This was carried out for the winter and summer seasons from 2009 to 2013 over North America and three sub-domains, as shown in Fig. 2.6 as can be seen in Fig. 2.2a, the spatial distribution of the observations network differs between these

sub-domains, being relatively uniform over the CONUS region, while over Canada most of the observations are located near the US-Canada borders. A high concentration of stations can be seen in southern Alberta and Saskatchewan: they are part of a network of automated agro-meteorological stations used as conventional observations. These three regions differ also in their winter snow/ice. A comparison of different CRCM5 simulations against ERA-Interim in model space (grid to grid comparison) has been also done to examine any differences from our verification approach.

Fig. 2.7 shows the average of the departures with respect to 2m surface temperature evolution for the period 2009-2013 in winter (Fig. 2.7a) and summer (Fig. 2.7b) seasons over North America and the three sub-domains mentioned above. In wintertime, CRCM-ERA and CRCM0.22-ERA have both a similar mean bias varying between 0 and -2 K over all domains, with a roughly constant cold bias of −2 K over North America. Being driven by ERA-Interim, these two simulations are constrained to remain relatively close to the observations. However, the CRCM-MPI and CRCM-CAN simulations can present different weather conditions than what was observed, which creates a more important departure with respect to observations. This is normal, since GCM-driven simulations are not expected to have their natural variability synchronized with that of the real-world climate trajectory. Hence, CRCM-MPI shows a variable average bias from one domain to another but is still always negative, varying from 0 to -3 K. CRCM-CAN presents also a variable cold bias between 0 and -3K over most regions except for a peak of warm bias of +1 K in 2011 for North America (CONUS and Canada). Bias noted in ERA-INT is related to the ability of ERA-Interim to reproduce the observed temperature, since observations are assumed to be verified and unbiased. A systematic nearly zero bias is noted over CONUS. However a warm bias of +1 K is present over Canada and the Arctic, which is not present in summer. Simmons and Poli (2014) pointed out that indeed ERA-INT has a warm bias in stable wintertime conditions over snow and ice in Arctic regions. This is in agreement with results discussed above where warm biases are observed

only in winter and over Canada and Arctic regions which are for the most part covered by snow-ice at that time of year.

In summertime, averaged bias scores are lower than in winter. On average, CRCM-ERA and CRCM0.22-ERA simulations have a mean departure with respect to observations that does not go below -1 K, being slightly better for the CRCM0.22-ERA experiment. CRCM-MPI is definitely colder than the observations by about -1 K to -2 K over the different regions. However CRCM-CAN is warmer than the observations over CONUS and Canada and presents a weak bias varying between ± 0.5 K over the Arctic. ERA-INT agrees relatively well with the observed 2-m temperature over all regions in summer.

To examine possible differences between the comparisons of climate simulations against raw observations in observation space and against ERA-Interim in model space (grid-to-grid comparison), the evolution of near surface temperature mean bias in model space is plotted in Fig. 2.8 in wintertime only, because this is the season where large climate variability is observed for the four regions. Fig. 2.7a represents $\overline{\left(H(\mathbf{X}_{ERA})-\mathbf{y}\right)}$ and $\overline{\left(H(\mathbf{X}_{Sim.})-\mathbf{y}\right)}$ where $\mathbf{X}_{ERA}$ and $\mathbf{X}_{Sim.}$ are respectively the ERA-interim reanalysis and any of the four climate simulations of Table 2.2 Therefore a comparison with respect to ERA-interim in model space is such that:

$$\overline{\mathbf{X}_{Sim.}-\mathbf{X}_{ERA}} \ .$$

Overall the same bias evolution pattern is then observed as in Fig. 2.7a except in some years where biases change sign particularly for CRCM-MPI and CRCM-CAN. However the sign of the bias remains negative if averaged over the five winter seasons. It is over CONUS that the mean bias evolution patterns from the two comparison methods are closer, confirming that the uniform observation coverage over CONUS represents well the observed climate.

RMSE is used to describe the variability of errors in ERA-INT and CRCM5 simulations experiments. It is important to keep in mind that the RMSE can be

decomposed into both the square of the bias and the variance of the error (Kabela *et al.*, 2015). The evolution of the RMSE in the period 2009-2013 over the different regions in both seasons is shown in Fig. 2.9. In wintertime (Fig. 2.9a) RMSE evolution over Canada and Arctic presents the largest difference in terms of variability against observations between simulations driven by ERA-interim and by CGCMs, but over CONUS RMSE values are comparable especially over the three first years of the study period. In summertime, the RMSE evolution (Fig. 2.9b) curves are close to each other for all CRCM5 simulations which means that the CRCM5 simulations variability of 2m temperature compared to the observation is smaller in summer than in winter and the lowest RMSE are observed over CONUS.

Those results reveal that in CRCM5 simulations, there are large errors in 2-m temperature with respect to raw observations are located over Canada and the Arctic in both seasons. However, the variability between CRCM5 simulations is larger in winter especially over Canada and the Arctic which explains in part why ERA-INT presents smaller RMSE then GCMs-driven simulations.

Fig. 2.10 displays the spatial distribution of the bias in 2-m temperature averaged for the two seasons during the period 2009-2013 and aggregated into a grid with a horizontal resolution of 0.5°. In wintertime (Fig 2.10a), ERA-INT shows a warm bias varying between 0-3 K over most parts of Canada and the Arctic particularly over Alberta and Saskatchewan. This bias is generally weaker in summertime and it is consistent with the spatial average bias evolution analysis discussed earlier.

For the other simulations, in winter, the spatial distribution of the 2-m temperature bias displays a cold bias over most parts of North America. It is strongest in the case of CRCM-MPI, reaching -6 K over the Canadian Prairies, the Mid-West and South West of CONUS. A cold bias is also seen in CRCM0.22-ERA over the Canadian Prairies but is slightly weaker than in CRCM-ERA. In summer, a strong warm bias of about +4-5 K is noted over the same regions in CRCM-CAN which can be explained

by the overestimation of SST in the CanESM2 model (Fig. 3a in Separovic *et al.*, 2013).

The climate simulations exhibit different behaviors in summertime, as shown in (Fig. 2.10b). CRCM-ERA and CRCM0.22-ERA have a warm bias over the Prairies reaching a maximum of +4 K, while elsewhere a small cold bias is noticed. In CRCM-MPI the bias is very small over the Prairies but a cold bias of -1 to -4K is present over most part of Québec, Ontario and CONUS but not over the West Coast of the United States where a warm bias is noted. According to Fig. 3b in Separovic *et al.*, (2013), this could be attributed to a warm SST bias in CRCM-MPI and CRCM-CAN compared to ERA-Interim. CRCM-CAN presents a strong warm bias reaching +5 K over the Great Plains and U.S Pacific coast, which could be attributed to the large warm bias over most part of the continent found in CanESM2 (Separovic *et al.*, 2013) which is transferred to the CRCM-CAN. A cold bias between 0 and -3 K is observed over most parts of Mexico in all CRCM5 simulations.

In summary, the direct comparison of CRCM5 simulations against 2m temperature observations shows roughly a lot of similarity to what is obtained when CRCM5 simulations are compared to ERA-Interim or gridded-data sets like CRU TS3.10 and Udel as shown by Martynov *et al.*, (2013) and Separovic *et al.*, (2013), even though our study is over a much shorter period than theirs (1989-2008). However, due to climate variability, the amplitudes of the biases for a particular season can vary in time depending on the simulation, the region and the year. Our results confirmed those found by many authors (Separovic *et al.*, 2013, Martynov *et al.*, 2013) who indicate that the performance of CRCM5 simulations is strongly sensitive to lateral boundary conditions and the forcing at the surface.

2.6 Comparison with radiosondes observations

The vertical structure of CRCM5 simulations and ERA-Interim will be now examined with respect to radiosondes. As the climate at the surface is the result of the interaction of several dynamical and physical processes in the upper levels, changes in precipitation, clouds and albedo depend on temperature, moisture and wind profiles. The evaluation of RCM's simulations in the vertical can provide an estimation of errors in radiation schemes used and atmospheric composition (Forster *et al.*, 2011). This can also provide an indication regarding the links between temperature profiles and storm characteristics like the potential intensity and frequency of Tropical cyclones (Gabriel *et al.*, 2012).

Fig. 2.11 presents the results of the comparison of CRCM5 simulations and ERA-INT against radiosonde observations over North America and over the three sub-domains considered. It shows the averaged vertical temperature bias over the four regions for winter and summer. ERA-INT has the same behaviour over all regions and both seasons with a good fit to observations and a bias near zero from 900 hPa up to 250 hPa over all regions. According to Simmons *et al.* (2014) a warm bias of about 0.5 K is noticed in the 250-150 hPa layer and can be related to the assimilation of warm-biased temperature data from commercial aircraft, particularly over North America (Dee and Uppala, 2009). Over CONUS in wintertime, CRCM-ERA and CRCM0.22-ERA present a small cold bias less than −1 K which is similar to the ERA-INT behaviour. However, CRCM0.22-ERA performs better than CRCM-ERA over most regions. In the same season, CRCM-MPI exhibits a cold bias between -1 to -2 K on average from the surface up to 300hPa which becomes stronger and exceeds -4 K over Canada and the Arctic above 300hPa. This cold bias at upper levels is increasing from south to north as we move from the United States, to Canada and then Arctic.

This behaviour of CRCM-MPI over North America is confirmed by a comparison of the zonal mean of the difference in temperature between the different CRCM5 simulations and ERA-interim in wintertime (Fig 2.12. These show a cold bias in CRCM-MPI at 50°N at the 200 hPa level and it extends to upper levels moving northwards. According to Stevens *et al.* (2013), a cold bias with respect to ERA-interim in the lower stratosphere is a characteristic of ECHAM6, the atmospheric circulation model of the MPI-ESM model. This cold bias at upper levels seems to be transferred from MPI-ESM to CRCM-MPI. Fig. 2.12b shows that beyond 200hPa CRCM-CAN exhibits an increasing warm bias over all regions reaching +4 K at 100 hPa, the same warm bias that was observed when comparing zonal temperature with ERA-Interim. This is due to the significant zonal-mean temperature bias from 200 to 7 hPa reported by Scinocca *et al.* (2008) in the fourth-generation atmospheric general circulation model CanAM4 used by the CanESM2 driven CRCM-CAN experiment.

In summer (Fig. 2.11b), CRCM-ERA and CRCM0.22-ERA vertical temperature profiles have a bias of ± 1K depending on vertical levels and regions; however CRCM0.22-ERA performs better than CRCM-MPI over Canada and the Arctic. CRCM-MPI displays a similar performance as in winter and has a comparable bias to simulations driven by ERA-Interim between surface and 300-200 hPa, but still suffers from a large warm bias in upper levels like in winter.

To examine the consistency of those results to those obtained by comparing CRCM5 simulations against ERA-Interim in model space, Fig. 2.13 presents a comparison of vertical temperature profiles differences between CRCM5 simulations with respect to ERA-interim in winter averaged over North America. The mean temperature biases for CRCM5 simulations are mostly the same as those estimated from the comparison to radiosondes, except for CRCM0.22-ERA where no difference is noted with respect to CRCM-ERA, which could probably attributed to the difference in horizontal resolution between ERA-interim (0.75°) and CRCM0.22-ERA, since ERA-Interim cannot reproduce extreme values at high resolution. A direct comparison to radiosondes is more revealing then.

Fig. 2.14 shows the RMSE of CRCM5 simulations and ERA-INT temperature profiles verified against radiosondes in both winter and summer. The RMSE of ERA-INT is less than 0.5 K over most of the atmospheric column in both seasons, except in a thin lower layer slightly above 1000 hPa level over Canada and the Arctic. This can be explained by a deficiency in the planetary boundary layer over those regions particularly in winter. The signature of warm bias in ERA-INT due to aircraft observations near 300hPa discussed above appears also in this figure. In wintertime, two distinct groups of profiles are associated with simulations driven by ERA-INT and simulations driven by the two CGCMs. The RMSE of CRCM-CAN and CRCM-MPI are nearly twice as large as the RMSE of CRCM-ERA and CRCM-CAN, indicating that simulations driven by CGCMs present larger errors and more variability with respect to the observations than simulations driven by ERA-Interim. The difference between the two groups could be interpreted as a measure of climate variability

In summertime, Fig. 2.14b shows that the RMSE for all CRCM5 simulations is lower than in winter. CRCM-ERA and CRCM0.22-ERA still remain the closest to the observations but the difference between the two groups is not as important as in winter season. The striking feature is that for CRCM-CAN and CRCM-MPI, they are now closer to the CRCM5 experiments driven by ERA-Interim, this is an indication of the lower variability in the boreal summer than in winter.

Looking at relative humidity, Fig. 2.15 presents vertical profiles of the averaged bias of CRCM5 simulations and ERA-INT in both seasons. It is important to keep in mind that the atmospheric moisture assessment is very complicated because of its small scale spatio-temporal variability which is significantly affected by atmospheric dynamics like convection and advection. Moreover, the poorness in the spatial coverage and temporal frequency (twice per day) of radiosonde measurements particularly does not cover oceans where the main source of atmospheric moisture is located (Trenberth *et al.*, 1998). Only averaged profiles over North America domain are shown because profiles over the other sub-domains display a similar behaviour.

The averaged profiles are only plotted up to 300 hPa level because beyond this level, relative humidity radiosonde measurements suffer from inaccuracy issues in cold and dry conditions in the upper troposphere (Miloshevich *et al.*, 2001).

In wintertime, all CRCM5 simulations except for the CRCM0.22-ERA in the 900-700 hPa layer are wetter than radiosondes observations by about 0 to +4% up to 500 hPa. CRCM-ERA and CRCM0.22-ERA simulations show the smallest relative humidity biases even compared to ERA-INT particularly in the mid-tropospheric levels. Above 700 hPa, all CRCM5 simulations and ERA-INT biases increase quickly with altitude and converge to approximately the same values at high altitudes.

In summertime, biases are larger and present more variability than in wintertime for all CRCM5 simulations. However ERA-INT keeps approximately the same bias as in winter. CRCM0.22-ERA and CRCM-CAN present the smaller biases varying respectively between 0 to +3% and 0 to +6% in the 1000-800 hPa layer. CRCM-ERA and CRCM-MPI have larger biases reaching more than +10% in the case of CRCM-MPI in the same layer. In the middle layers between 800-600 hPa, all CRCM5 simulations exhibit a dry bias reaching -3% which increases, changing sign in the upper layers and converging to the same values at high levels.

In both seasons, all CRCM5 simulations and ERA-INT are wetter than radiosonde observations over most of the tropospheric column, which produce more precipitations. This can explain some results found by Separovic *et al.* (2013) and Martynov *et al.* (2013), who showed that simulated precipitations by various CRCM5 simulations are overestimated over most of North America especially in winter during the period 1989-2008. Fig. 2.16 displays the RMSE of relative humidity vertical profiles in both seasons. In wintertime, CRCM-ERA and CRCM0.22-ERA show a RMSE less than that of CRCM-MPI and CRCM-CAN by about 4% which tends to be reduced with altitude up to 500 hPa. However, in summer, the RMSE is closer for all simulations except for CRCM-MPI which exhibits a very large error between the surface and 800 hPa reaching 13.5%. The other simulations show an increased RMSE

from surface to 900 hPa up to 9% and then decreased to 5% at 500 hPa. In both seasons, beyond the 500 hPa level, the RMSE increases quickly for all CRCM5 simulations and ERA-INT and tend to converge to the same values.

2.7 Comparison with satellite observations

Until recently and despite the development of instruments and telecommunication technology, there is still a lack of direct meteorological observations over oceans, the polaes and desertic regions. Satellite observations provide a quasi-complete global coverage with reasonable spatial and temporal resolutions over those regions. This allows satellite observations to be an alternative as reference datasets to assess temperature and humidity profiles from climate models (John and Soden, 2007) or for the monitoring of important climate variables like sea surface temperature (Reynolds *et al.*, 2002).

Satellite observations could be a good substitute to radiosondes observations in the upper troposphere, because as mentioned in Section 2.6 and in many other studies, radiosonde measurements, particularly the moisture in the upper troposphere at very cold temperatures, can suffer from significant biases (Miloshevich *et al.*, 2001; Sapucci *et al.*, 2005). However, as the weighting functions shown in Fig. 2.4 and Fig. 2.5 indicate, each channel only represents a measurement representative of temperature or water vapour content averaged over a broad layer.

In this section, microwave radiances from the AMSU-A and AMSU-B satellite instruments (Table 2.2) have been used as a reference dataset to assess upper troposphere temperature and water vapour respectively. Those are expressed in terms of brightness temperatures (in deg K) which is the temperature, a black body should have to emit that radiance. Only clear sky radiances are used because the observation

operator is not at the moment able to include satisfactorily the effect of clouds in the radiative transfer model (Buehler *et al*, 2007; Chouinard and Hallé, 2003).

*2.*7.1 Upper tropospheric temperature

Spatially averaged observed brightness temperatures aggregated to 0.5°×0.5° grid resolution from AMSU-A Channel 7 and 8 are presented in Fig. 2.17, showing that brightness temperatures for Channel 7 are warmer than those of Channel 8. This is consistent with the vertical temperature weighting function in the troposphere, from Fig. 2.4, indicating that Channel 7 peaks below Channel 8 where temperatures are much warmer. Moreover, AMSU-A observations capture the seasonal temperature variation between winter and summer seasons. Due to the uncertainty of surface emissivity over land in the microwave bands (Chouinard and Hallé, 2003), some data were rejected by the data selection of the data assimilation system, where the contribution from the surface may be non-zero due to the topography elevation as over the center of Greenland, the Rocky Mountains and the western Sierra Madre. Those areas are shown in white in Fig. 2.17a, indicating that no radiance measurements were available. As can be seen in Fig. 2.17b for Channel 8, all areas are filled because there is no radiative contribution from the surface that can affect radiance measurements for this channel.

Fig. 2.18 displays winter and summer seasonal averaged brightness temperature bias for ERA-INT and CRCM5 simulations with respect to AMSU-A Channel 7. The radiative transfer model, RTTOV is used to produce the model-equivalent of radiances given the current model state (e.g., profiles of temperature and humidity) for the period 2009-2013. Those can then be directly compared to the same observed data of the corresponding channels of AMSU-A, B. Channel 7 being sensitive to a

layer centered at 300hPa level (Fig. 2.4), the radiance measured by this channel comes to a large extent from a layer centered at the peak of the weighting function of this channel.

In both seasons, ERA-INT is in good agreement with AMSU-A radiances of Channel 7 where a constant bias near zero bias is observed over the entire continent. This is expected since AMSU-A data were assimilated in ERA-interim (Dee and Uppala, 2009). CRCM0.22-ERA and CRCM-ERA present a small bias of about ±1 K over most part of the continent except for CRCM-ERA in summer where a warm bias between 1 and 2 K is noted over the Labrador Sea.

CRCM-MPI reveals a strong cold bias pole north of the 60th parallel reaching -6K in winter. This cold bias near the pole is weaker in summer and shifts toward Alaska and the North-West regions of Canada. Elsewhere, the bias varies between 0 and -2 K which is in agreement with results found in Section 2.6 where a cold temperature bias was observed when comparing CRCM5 simulations to radiosondes (Fig. 2.11) and when comparing temperature against ERA-Interim (Fig. 2.12), a cold bias emerges North of 50N and above 300 hPa.

CRCM-CAN has a warm bias over North America in both seasons. In wintertime a significant warm bias of 3 to 4 K is noted over the Canadian Archipelago and Hudson Bay while in summertime the warm bias over the North pole shifts eastward over the Labrador sea and Greenland becoming weaker than in winter. Over other regions, the bias varies mainly between 0 and 2 K in both seasons. This is consistent with results discussed in Section 2.6 where the temperature bias of CRCM-CAN over the Arctic presented an increasing positive bias above 300 hPa (Fig. 2.11). A warm bias is noted above 200 hPa when comparing zonal vertical temperature with ERA-Interim (Fig. 2.12).

Fig. 2.19 is similar to Fig. 2.18 but for AMSU-A Channel 8 as reference. The peak of the weighting function of this channel is above the peak of channel 7 at about

200 hPa level (Fig. 2.4). The conclusions drawn from the comparison to Channel 7 apply also to Channel 8.

Fig. 2.20 displays the evolution over the five years of the study of the observed and model equivalent of brightness temperatures for Channels 7 and 8 of AMSU-A. These have been seasonally averaged over North America for each of the five years. The averaged brightness temperatures from satellite observations and CRCM5 simulations have a seasonal variability. For both channels and seasons the simulated brightness temperatures CRCM-ERA fit very well the satellite observations, having roughly the same evolution as the satellite observations. This can be related to the fact that it is driven by ERA-Interim and its resolution of 0.44° is comparable to the resolution of satellite radiances which is 45km. However, CRCM0.22-ERA displays a systematic difference over the five years of about 2-3 K in winter and about 1 to 2.5 K in summer for both channels; this difference is potentially explained by extreme values of climate variables simulated by CRCM0.22-ERA at 0.22° horizontal resolution, which are not caught by satellite observations. CRCM-MPI mean brightness temperature bias presents a negative difference about 3-4 K in wintertime and 2.5 K in summertime for both channels. CRCM-CAN reveals a relatively constant difference varying between 2-3 K with respect to satellite observations for both channels and seasons. This means that, on average, the thermal state in the upper troposphere of CRCM-MPI and CRCM-CAN are respectively colder and warmer than satellite observations, which is in agreement with results found with the comparison to radiosondes observations discussed previously in Section 2.6.

2.7.2 Upper Tropospheric Water Vapour

Water vapour in the upper atmosphere is very important in climate studies because of its strong greenhouse effect contributing for 50% of present-day global greenhouse

effect (Schmidt *et al.*, 2010). It absorbs and emits radiation across the entire infrared spectrum, which is a critical part of the Earth energy budget. GCMs and RCMs must therefore simulate accurately water vapour transport and distribution to provide a reliable estimation of climate and climate changes.

Brightness temperature from AMSU-B Channel 3 at 183 GHz is strongly correlated to the mean relative humidity between 500 and 200 hPa (Milz *et al.*, 2009). Buehler *et al.* (2008) have noted that a brightness temperature difference of 1 K corresponds approximately to a relative change in upper tropospheric mean relative humidity in the layer 500-200 hPa of approximately 7%. Several studies have used satellite observations to assess the moisture balance in GCMs Upper Troposphere Water Vapour (UTWV). Iacono *et al.* (2003) succeeded to capture the variability of UTWV over the Pacific Ocean during an El Niño event by using the High-Resolution Infrared Radiation Sounder (HIRS) satellite observations. Allan *et al.* (2003) assessed the simulated distribution and variability of UTWV from the Hadley Centre Climate Model against brightness temperatures in water vapour channel from HIRS.

Water vapour absorbs microwave radiation at the frequency of AMSU-B Channel 3. The data from this channel can be used here to examine and evaluate UTWV of ERA-INT and CRCM5 simulations. If water vapour content increases in the upper troposphere, microwave radiation from Earth will be absorbed and less radiation can reach the satellite. Low (high) values of brightness temperature then indicates areas of relatively high (low) water vapour content.

Fig. 2.21 shows the observed mean seasonal brightness temperatures from AMSU-B Channel 3 in winter and summer seasons over North America. The analysis will focus on sub-tropical and tropical regions to prevent radiance contamination due to surface effects due to the extremely dry atmospheric conditions (Buehler and John, 2005). The figure shows that the water vapour content is higher in winter than in summer in subtropical regions, which can be explained by the fact that, in wintertime, the UTWV pattern is governed by the general atmospheric circulation which is more

active in winter than in summertime. Subsidence tends to dry the upper troposphere while ascent moistens it. In summertime, an area of high UTWV is noticed over the Caribbean Archipelago which can be related to the vertical transport of moisture from surface to upper levels by deep convection process, which is very active over this region. The observed UTWV pattern in both seasons displayed in Fig. 2.21 is in agreement with patterns found by Iacono *et al.* (2003) using HIRS observations.

Fig. 2.22 shows the spatial distribution of the difference between the AMSU-B channel 3 data and the model equivalent obtained by the radiative transfer model RTTOV from CRCM5 simulations and ERA-INT in both seasons. Positive (negative) differences represent warmer (colder) brightness temperatures of the simulated than the observed data which then corresponds to a dryer (moister) area in the simulations compared to the observations.

As expected, ERA-INT exhibits very small brightness temperature differences in both seasons. In wintertime, CRCM-ERA and CRCM0.22-CAN show an area of cold brightness temperature bias of -2 K seen over the Caribbean Archipelago corresponding to an overestimation of UTWV content. For CRCM-MPI, a cold bias of about -3 to -4 K is observed over the Caribbean Sea and Canadian Arctic interpreted as too high UTWV produced by those simulations. In the same season, CRCM-CAN on the other hand shows the strongest brightness temperature biases of all simulations going from -6 to +6 K in the Tropical regions. The UTWV is hugely overestimated over the Caribbean Archipelago and East of Florida. Conversely, an area of largely underestimated UTWV is present off the West coast of Mexico. In summertime, the convection over Tropical regions is very active and a large area of high moisture related to a cold bias of -4 to -6 K is observed in all CRCM5 simulations over most part of CONUS, extending to the Tropical Pacific regions in the case of CRCM-MPI and CRCM-CAN. Finally, a strong warm bias of 2-4 K covers the Gulf of Mexico and the Caribbean Sea for all simulations indicating an underestimation of UTWV content over those regions compared to observations with larger and stronger dry area in CRCM-CAN.

It is difficult to determine exactly why the UTWV is overestimated or underestimated. A hypothesis could be given related to the deficiency in some dynamical component, particularly the CRCM5 convection scheme and the water vapor representation over in the atmospheric

The results indicate that the capability of different CRCM5 simulations to reproduce the observed UTWV pattern is variable from one simulation or region to another. Most differences with respect to the observations are noticed over the Tropical and subtropical regions, where convection is the main process of vertical transport from the surface to all altitudes of the troposphere.

Some difficulties could be encountered to interpret results from climate simulations using satellite observations, because climate simulations variables and satellite radiances have not the same units and dimensions, and should be converted into the same variable to make a fair and consistent comparison. To convert brightness temperature in « real » temperature, a ruile of thumb is that 1K in brightness temperature is equivalent to 0.1K of real temperature. This comes from the Planck function. However, the treatment of water vapor and cloud variables is the Achille's heel of current climate model. The point that needs to be made is that bias and relative humidity measured by comparing to radiosondes and to satellite radiances concur giving confidence that satellite radiances would be useful in areas where there are no radiosondes. For those reasons, more detailed studies are required to exploit the potential of using large and various satellite data-sets for RCMs validation and enhancing climate understanding.

2.8 Summary and conclusion

The performance of different CRCM5 simulations over the North American CORDEX domain for the period 2009-2013 has been assessed by a direct comparison to surface weather stations, radiosondes and satellite observations. This approach contributes in giving a new point of view about RCMs validation techniques, particularly by using satellite observations.

The observation operator of the CMC variational data assimilation system has been used to transform the CRCM5 simulations and ERA-Interim from model to observation space, this allows a direct comparison against observations that are consistent in terms of spatial sampling and variable type.

CRCM5 simulations and ERA-Interim have been compared with observed 2m surface temperature over North America and over sub-domains: CONUS, Canada and Arctic. An overall average bias of ± 2 K has been noted over the three regions in summer for all CRCM5 simulations, except over Canada where biases exceed this range for the CRCM-MPI and CRCM-CAN experiments. In winter, the simulations reveal mainly a cold bias over all domains except for CRCM-CAN which tend to be warmer during 2010 and 2011. The best simulations are CRCM-ERA and CRCM022.ERA followed by CRCM-CAN and CRCM-MPI. On the other hand, ERA-INT shows a systematic warm bias in winter of about 1 K over Canada and Arctic probably due to the presence of surface snow and ice. The direct comparison of CRCM5 simulations against with raw observation agrees with the results obtained in a comparison with ERA-Interim (in model space) particularly over CONUS, where surface observation stations are distributed most uniformly. Using the RMSE metric, it has been shown that simulations driven by CGCMs present a larger variability than those driven by ERA-INT in winter, except over CONUS where small values are noted, however during summer RMSEs are comparable for all CRCM5 simulations.

The temperature and relative humidity vertical structure of CRCM5 simulations and ERA-INT were then compared against radiosondes observations. As expected,

for, ERA-INT, the average temperature error exhibits a profile with a very small bias and a RMSE of about 0.25 K in both seasons and over all regions except for a small warm bias of 0.5 K near the 300-200 hPa layer. This confirms that ERA-Interim is the more reliable reference to assess vertical temperature of climate simulations and numerical weather prediction forecasts. However, climate simulations have a different behavior. CRCM-ERA and CRCM0.22-ERA have the best performance with an advantage for the last one, while CRCM-CAN and CRCM-MPI show a significant large RMSE especially during winter. The comparison of the vertical temperature profiles of CRCM5 simulations against ERA-Interim and radiosondes showed a good agreement between the two evaluation approaches (grid to grid and in observation space comparison), since both methods presents biases and RMSEs near zero.

The vertical distribution of relative humidity has been compared to radiosondes measurements. CRCM-ERA and CRCM0.22-ERA are relatively the best for relative humidity among all climate simulations, while CRCM-MPI and CRCM-CAN showed large biases and RMSEs. It has been shown in this study that ERA-Interim presents small biases and RMSE of vertical relative humidity regarding radiosonde observations at the lower and middle tropospheric levels and large values at upper levels, which may require improvements.

The comparison of upper tropospheric temperature between CRCM5 simulations and ERA-INT against Channel 7 and 8 of AMUS-A satellite observations shows a strong cold brightness temperature bias in CRCM-MPI and a warm one in CRCM-CAN over Polar Regions particularly in wintertime. These results are confirmed by comparing the same simulations against radiosondes and ERA-Interim. This shows the difficulties of those two simulations to reproduce the atmospheric thermal state in the upper troposphere. ERA-Interim, CRCM0.22-ERA and CRCM-ERA simulate well the observed brightness temperature pattern.

The moisture in the upper troposphere has been evaluated using Channel 3 of AMSU-B satellite observations. In both seasons CRCM0.22-ERA and CRCM-ERA

could reproduce reasonably well the observed AMSU-B Channel 3 pattern except in summer where the UTWV is overestimated over large regions of CONUS and is underestimated over the Caribbean Archipelago and the Gulf of Mexico. This could be explained by a deficiency in the convection process which are very active in this season and over those regions. CRCM-CAN and CRCM-MPI had difficulties to reproduce the observed pattern especially over the Tropical and Sub-tropical regions in both seasons (Iacono, 2003).

This study has shown the feasibility to assess RCMs simulations and reanalysis directly against independent raw observations using the observation operator of data assimilation system. It has been shown that the observed climate is not always equivalent to the analysed climate (reanalysis) particularly near the surface and in the upper troposphere. It was also shown that ERA-Interim reanalysis is a good substitute for upper air temperature observation over North America at least, but shows some weaknesses near the surface particularly over Canada and the Arctic. CRMC5 simulations driven by GCMs reflect the deficiencies of GCMs at surface and upper levels while simulations driven by ERA-Interim reanalysis presents the best performance. It was also shown that increasing the simulation horizontal resolution could improve the performance in the troposphere but not systematically near the surface.

Finally, using satellite observations as independent reference data-set to assess RCMs, they were shown to be very useful for studying upper air water vapor distribution, its impact on the earth radiation budget and assessing convective schemes, particularly over oceans and regions poorly observed.

Acknowledgments

The authors would like to thank Dr. Ping Du who provided the programs that made this study possible. Support from Mrs. Katja Winger and Mr. Michel Valin is also gratefully acknowledged.

This research was funded by the Grants and Contribution program of Environment Canada, Natural Sciences and Engineering Research Council of Canada (NSERC) Discovery Grant program, the Canadian Network for Regional Climate and Weather Processes (CNRCWP) funded through the Climate Change and Atmosphere Research (CCAR) program of NSERC and the "Ministère du Développement Économique, de l'Innovation et de l'Exportation (MDEIE) of the province of Québec. High performance computing resources were provided by Compute Canada on the Guillimin platform of the Calcul Québec regional consortium. The first author benefited from a scholarship from the Faculty of Science of the Université du Québec à Montréal (UQAM).

CHAPITRE III

CONCLUSION

La performance de différentes simulations climatiques du MRCC5 sur le domaine CORDEX Amérique du Nord durant la période 2009-2013 a été évaluée par une comparaison directe aux stations d'observation de surface, radiosondages et radiances satellitaires. Cette comparaison contre des données de référence indépendantes du pilotage utilisé dans le MRCs conduit à une comparaison plus précise des simulations MRCC5, particulièrement sur les régions où la distribution des stations d'observations de surface est régulière comme sur la partie continentale des États-Unis. La comparaison par rapport à des observations sur une grille (e.g., CRU et Udel) ou à des ré-analyses peut être entachée d'erreurs reliées aux méthodes utilisées pour la production de ces observations synthétiques.

L'opérateur d'observation du système d'assimilation de données variationnel d'Environnement Canada a été utilisé pour convertir les simulations MRCC5 et les ré-analyses ERA-Interim en équivalent-modèle des observations, permettant ainsi une cohérence spatiale et temporelle et une équivalence en termes de nature et dimensions des variables. Le Premier objectif de cette étude était d'évaluer le biais et l'erreur quadratique moyenne sur l'Amérique du Nord, la partie continentale des États-Unis, le Canada et l'Arctique des simulations MRCC5, une comparaison traditionnelle (grille à grille) par rapport aux ERA-Interim a été effectuée pour examiner les éventuelles différences entre les deux approches. Deux expériences ont été effectuées en utilisant le MRCC5 piloté par ERA-Interim à une résolution horizontale de 0.44° (CRCM-ERA) et une autre à 0.22° (CRCM022-ERA) pour évaluer l'impact de l'augmentation de la résolution horizontale sur la performance du modèle. Deux autres simulations ont été menées afin d'examiner l'impact du pilotage sur la

performance des simulations forcées aux frontières et en surface par des MCGAOs Le modèle CanESM2 a été utilisé pour l'expérience CRCM-CAN, et le modèle MPI-ESM-LR pour l'expérience CRCM-MPI.

Cette étude a montré la faisabilité de la validation des simulations MRCC5 contre des observations brutes et non conventionnelles comme les radiances satellitaires en utilisant l'opérateur d'observation. Il a été montré aussi qu'en comparant les simulations climatiques directement aux observations à partir des stations de surface et des radiosondages dans l'espace des observations, les mêmes conclusions sont obtenues en comparant les mêmes simulations contre ERA-Interim dans l'espace du modèle, particulièrement sur la partie continentale des États-Unis où le réseau d'observations est uniforme. Par contre quelques différences entre les deux approches ont été remarquées sur le Canada et l'Arctique en hiver qui peuvent être reliées à la non-homogénéité et à la représentativité des observations sur ces régions. En comparant aux radiosondages, les simulations CRCM5 pilotées par les deux MCGAOs, présentent de forts biais de température dans la haute troposphère. Ceci a été confirmé par l'utilisation des radiances satellitaires sensibles à la température de la haute troposphère, ce qui confirme la pertinence de l'utilisation des radiances satellitaires comme données de références indépendantes surtout sur les régions ou les observations conventionnelles sont rares ou inexistantes. Des différences significatives ont été observées entre les simulations pilotées par ERA-Interim et celles pilotées par les deux MCGAOs en terme d'erreur quadratique moyenne (EQM) en hiver, ceci peut être attribuées à la variabilité climatique des MCGAOs transférée aux simulations climatiques. Le pilotage de la simulation climatique MRCC5 avec ERA-Interim et l'augmentation de la résolution horizontale contribuent largement au rapprochement des simulations aux observations. Contrairement aux températures, les profiles de l'humidité relative des différentes simulations MRCCx 5 sont comparables en termes de biais et d'EQM, mais avec une faible amélioration pour les expériences CRCM-ERA et CRCM0.22-ERA.

Il a été montré dans cette étude, qu'ERA-Interim reproduit bien les températures observées en surface et en altitude, sauf en hiver où un biais chaud en surface d'environ 1 K a était constaté sur le Canada et l'Arctique due probablement à la présence de la neige ou de la glace en surface sur ces régions. Le profil d'humidité relative révèle des biais et des EQMs relativement faibles en basse et moyenne troposphère comparés à la haute troposphère qui est caractérisée par des grandes valeurs.

La vapeur d'eau dans la haute troposphère simulée par le modèle MRCC5 a été analysée en utilisant les radiances satellites AMSU-B Canal 3 exprimé en températures de brillance. Les résultats ont montré des différences significatives en termes de température de brillance observée et modélisée, entre les différentes simulations climatiques, particulièrement sur les régions Tropicales en été. Ces différences pourraient être reliées à une faiblesse dans la composante dynamique, au processus de la convection du MRCC5 ou à la mauvaise représentation de la vapeur d'eau dans la colonne atmosphériques. Des études plus poussées sont requises pour comprendre les causes de ces différences.

Il est recommandé d'explorer plus en détails l'utilisation du grand éventail des radiances satellitaires disponibles pour l'évaluation des performances des MRCs, et pour faire avancer la compréhension des différentes composantes du système climatique.

FIGURES

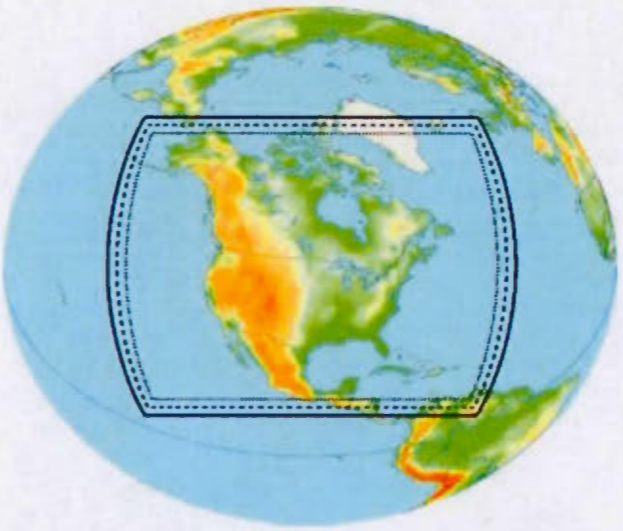

Figure 2.1 The CORDEX CRCM5 domain over North America

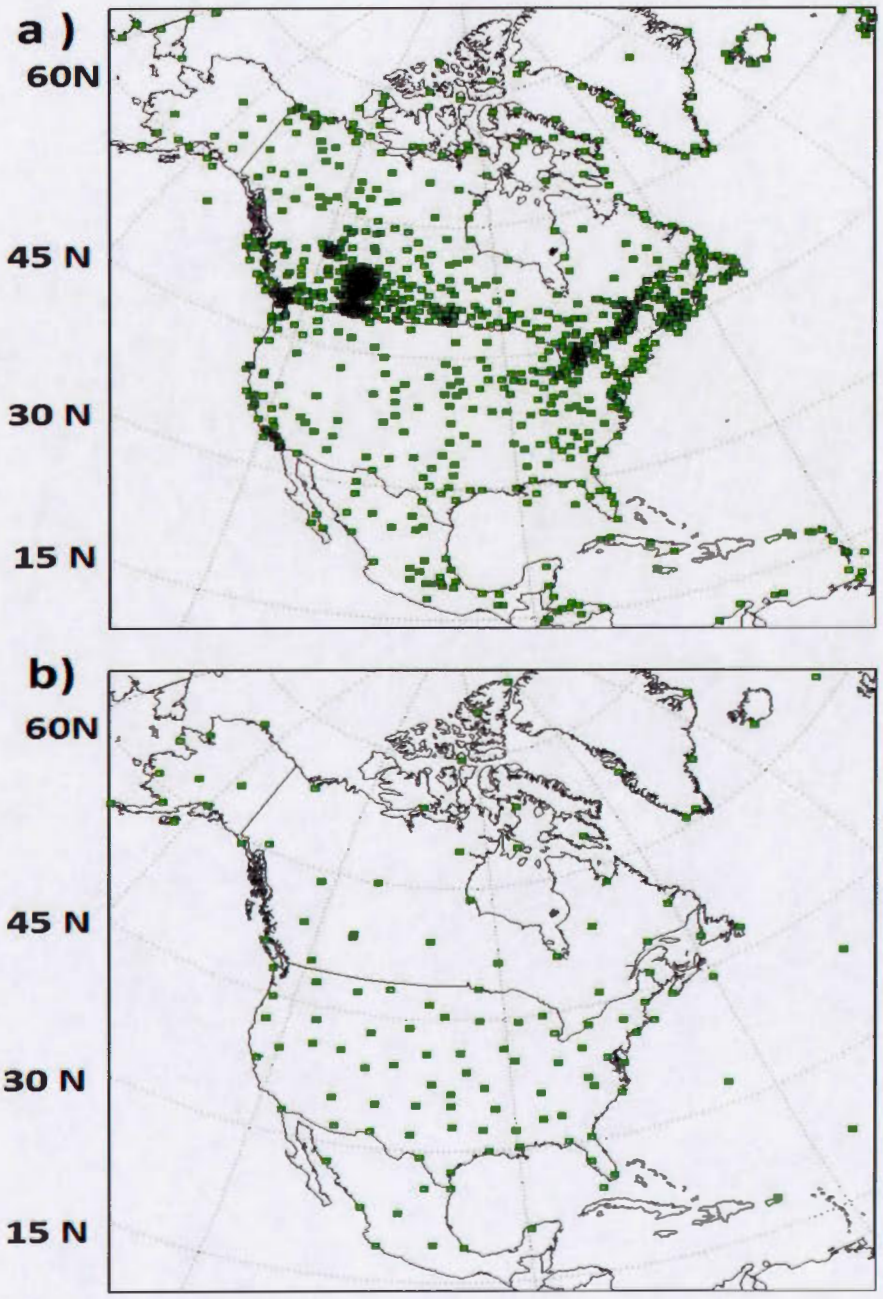

Figure 2.2 North America weather stations network for: a) surface and b) upper air observation

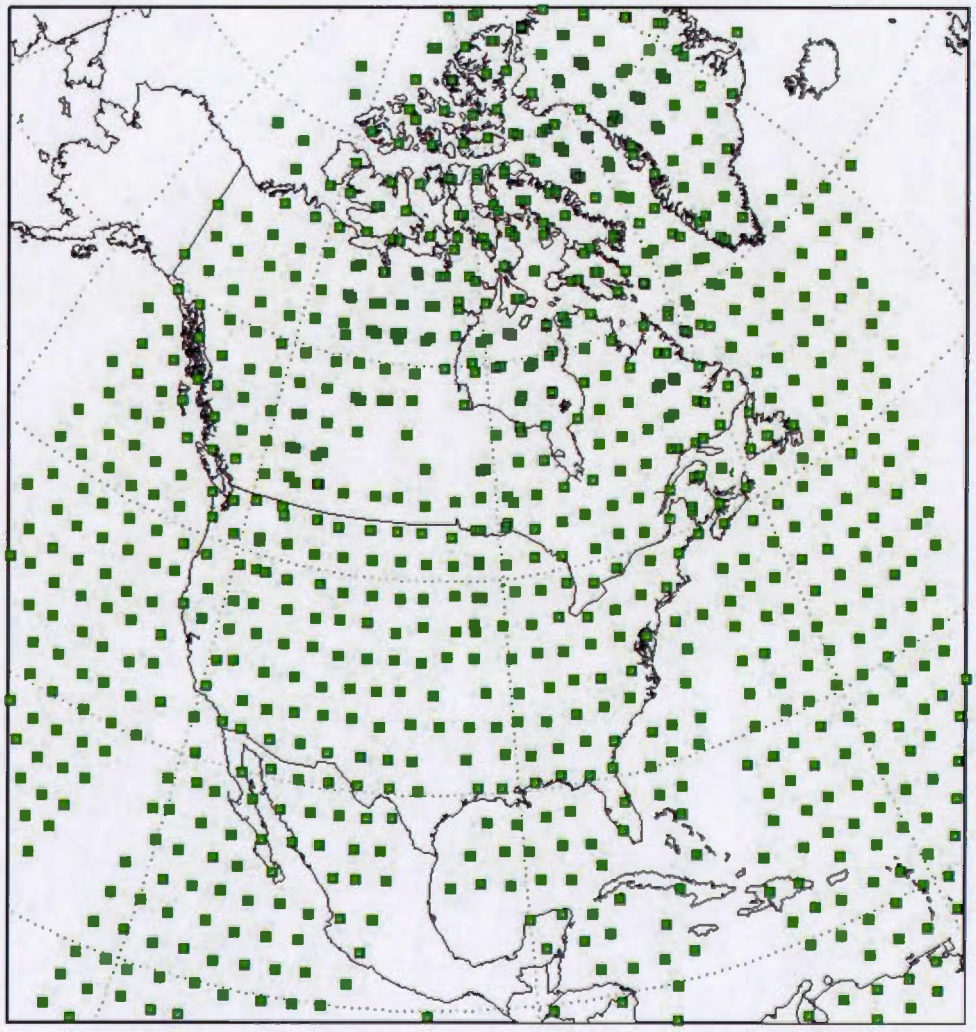

Figure 2.3 Spatial coverage of AMSU-A data over North America in 6 hours time window.

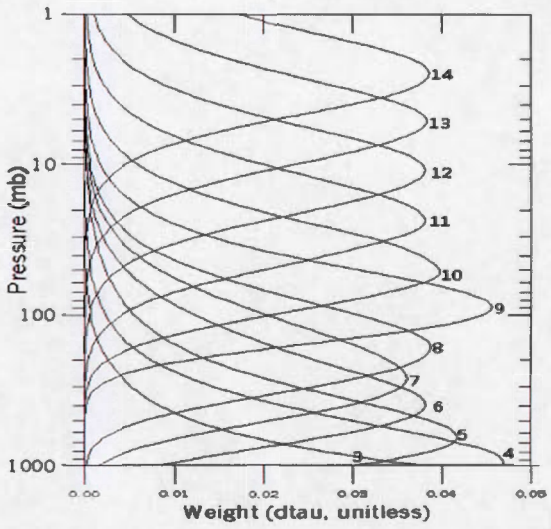

Figure 2.4 AMSU-A Channels weighting functions sensitive to temperature (From Kidder et al. 2000).

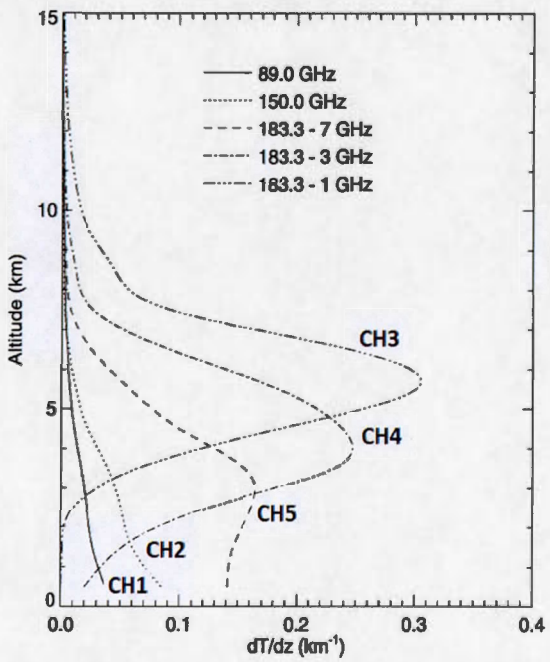

Figure 2.5 AMSU-B Channels weighting functions sensitive to water vapor (From Deeter and Vivekanandan 2005).

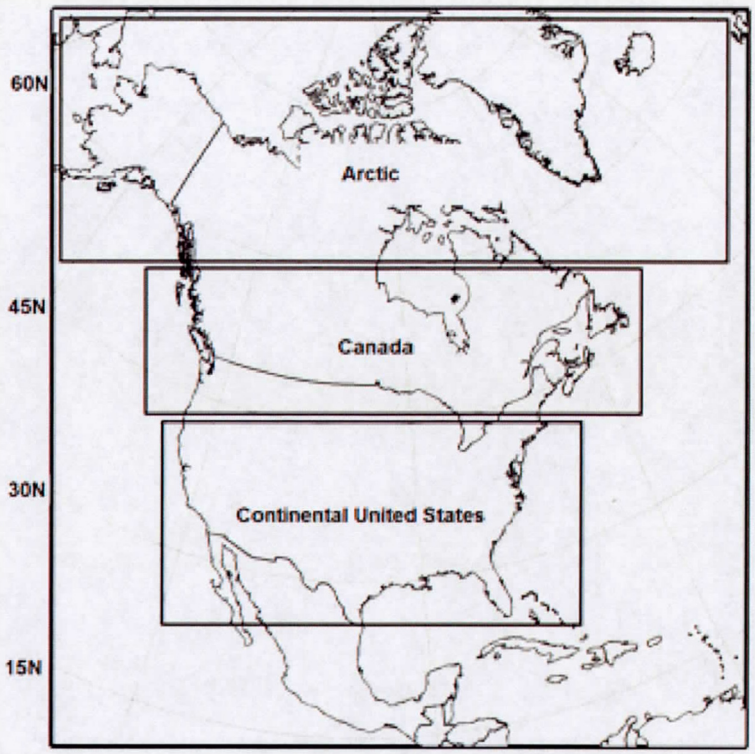

Figure 2.6 Sub-domains considered in the study.

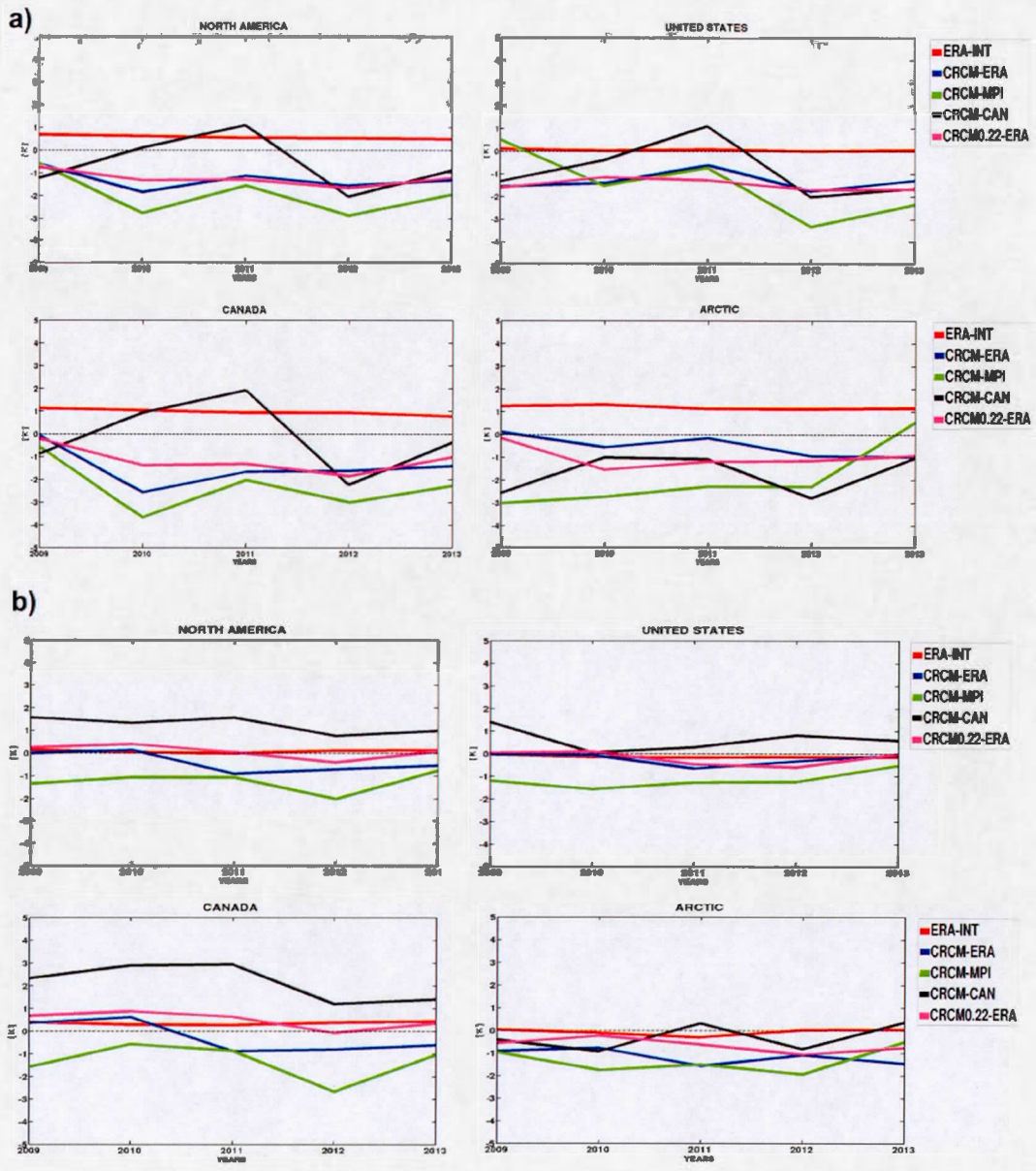

Figure 2.7 Average 2m temperature bias against evolution against observations over North America and the three sub-domains (United States, Canada and Arctic) in a) winter and b) summer season.

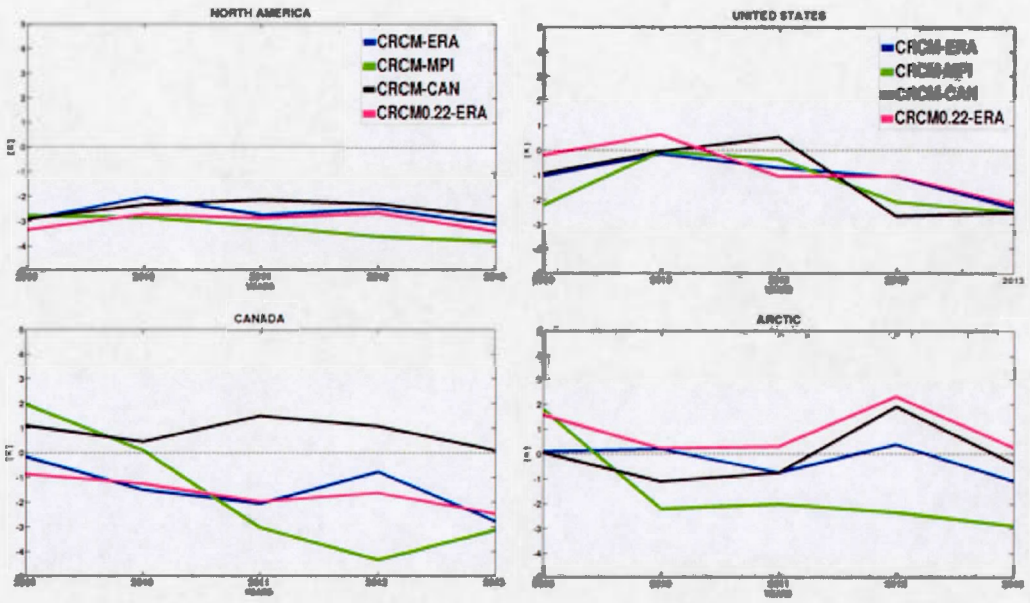

Figure 2.8 Average 2m temperature bias evolution against ERA-Interim evolution over the North America and the three sub-domains (United States, Canada and Arctic) in winter season.

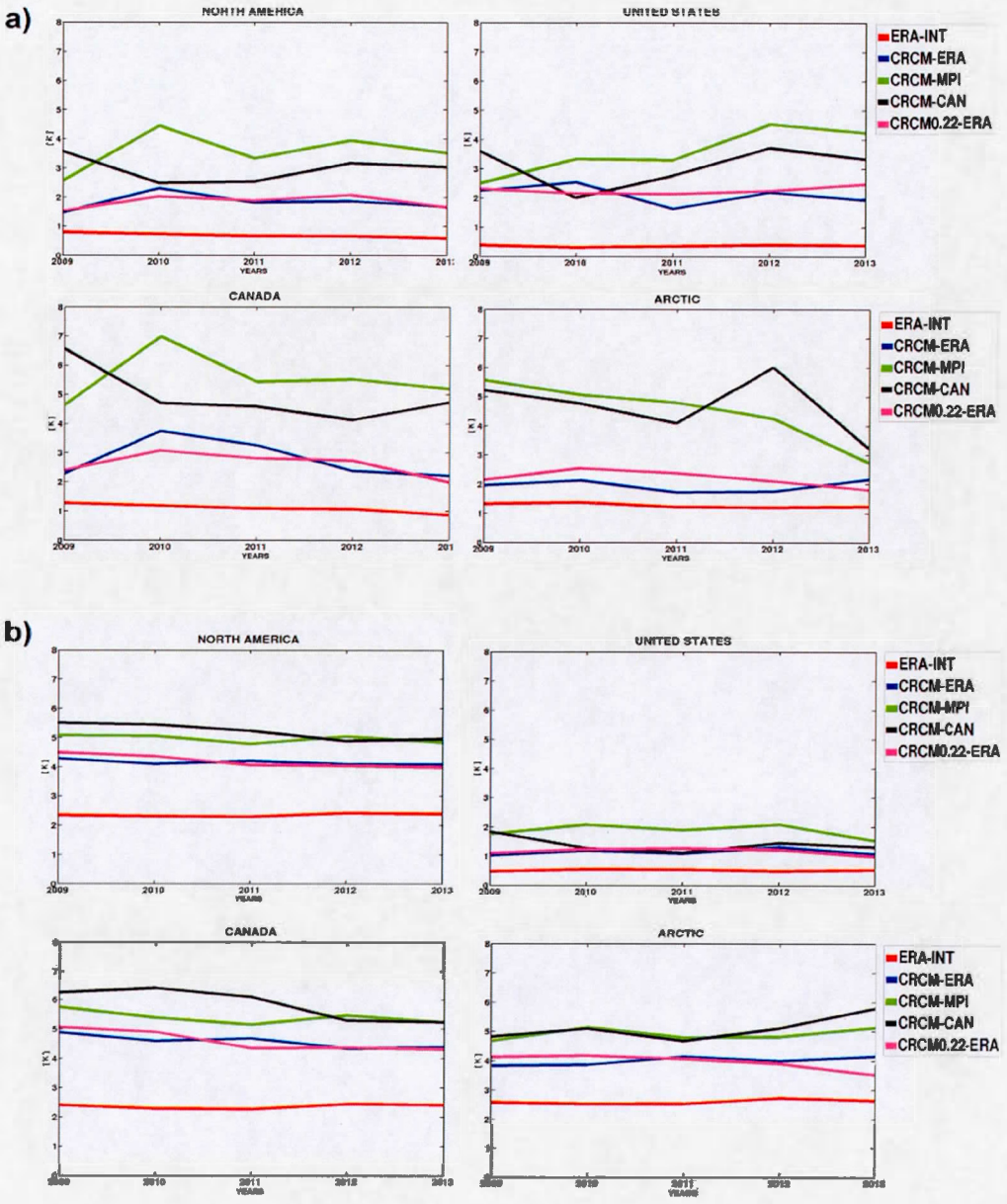

Figure 2.9 Average 2m temperature root mean square error evolution over the whole North America and the three sub-domains (United States, Canada land Arctic) in: a) winter and b) summer season.

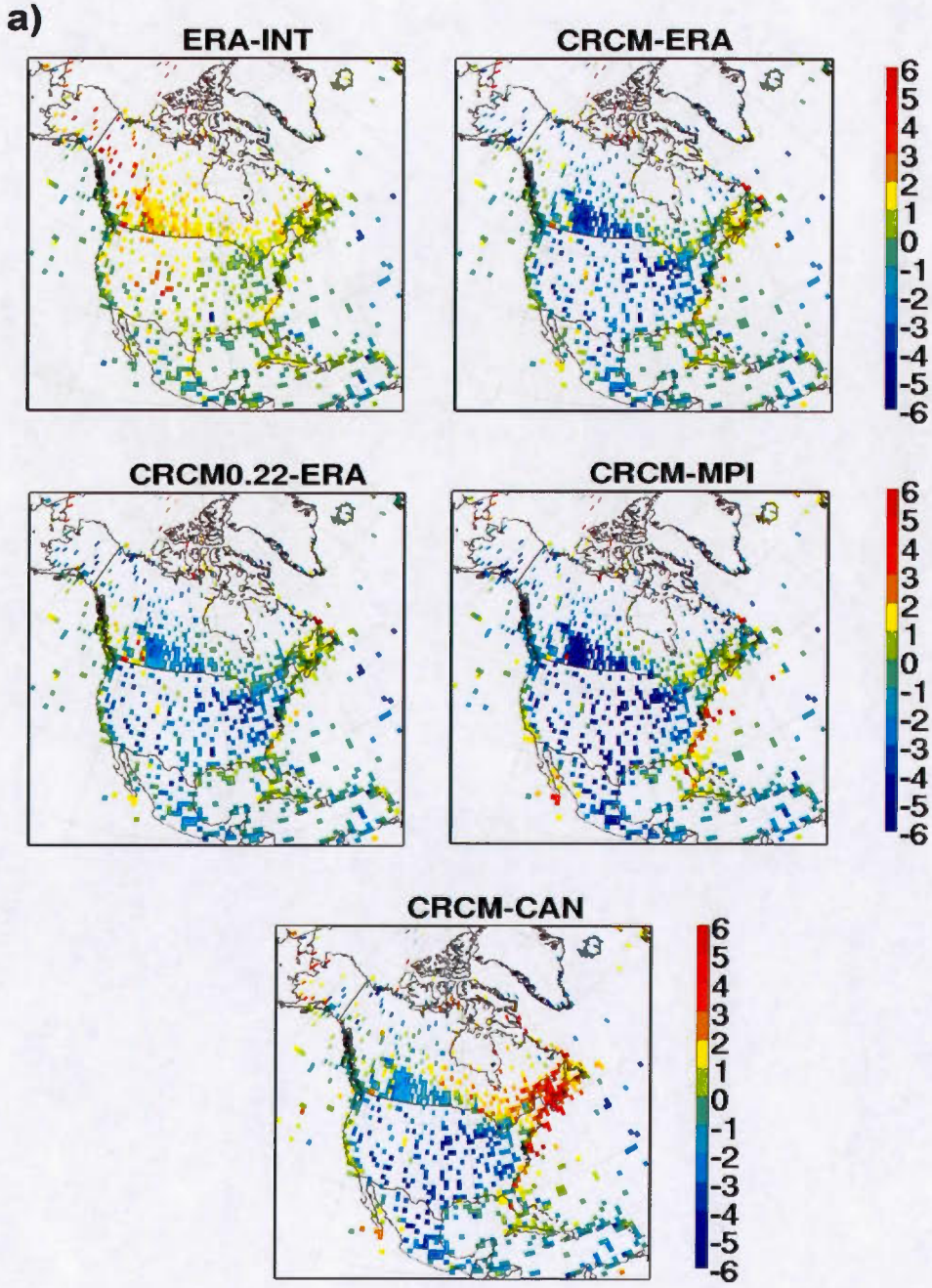
a)
ERA-INT
CRCM-ERA
CRCM0.22-ERA
CRCM-MPI
CRCM-CAN
6
5
4
3
2
1
0
-1
-2
-3
-4
-5
-6

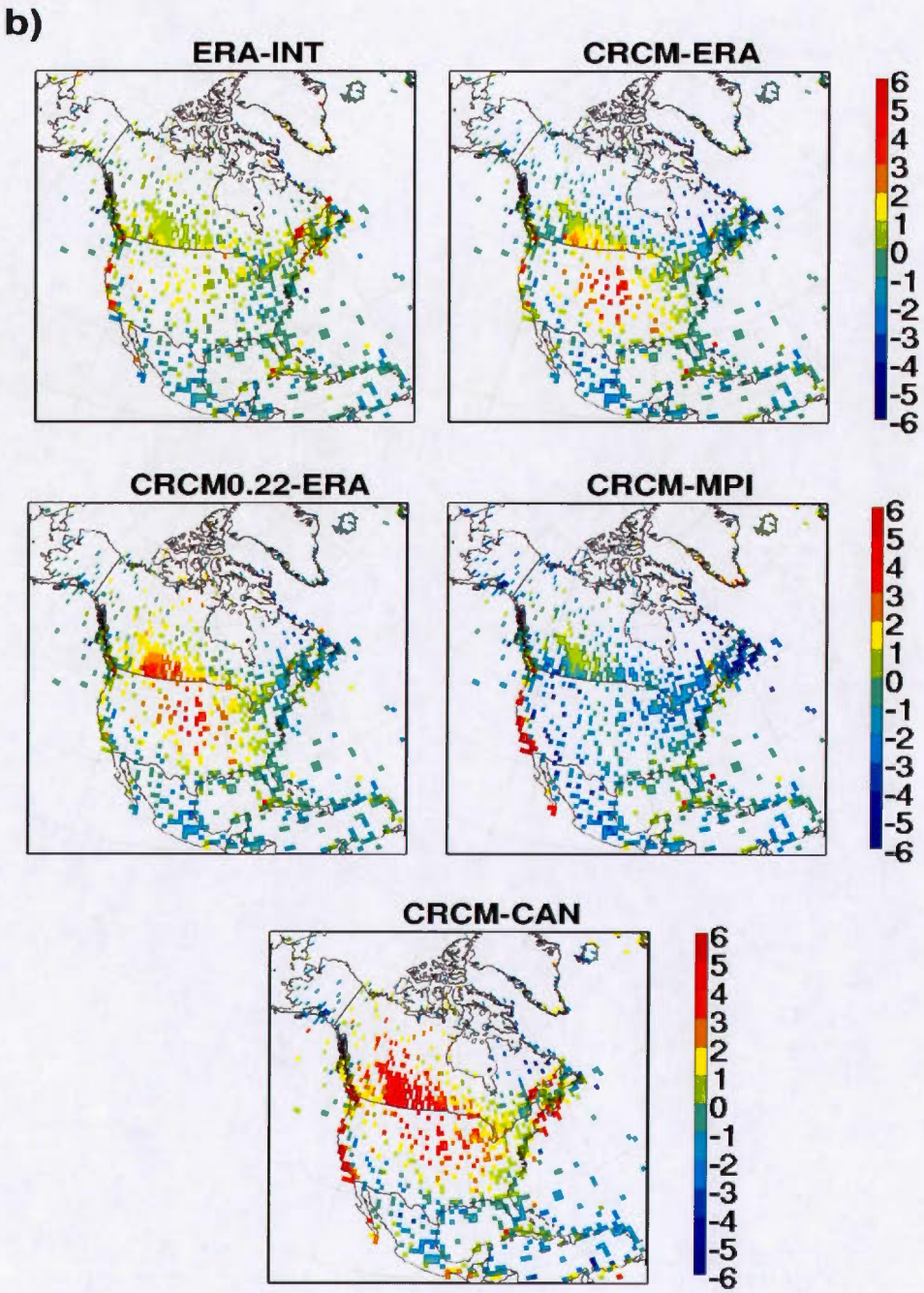

Figure 2.10 Spatial distribution of 2m temperature bias aggregated into 0.5° cells for: a) winter and b) summer season.

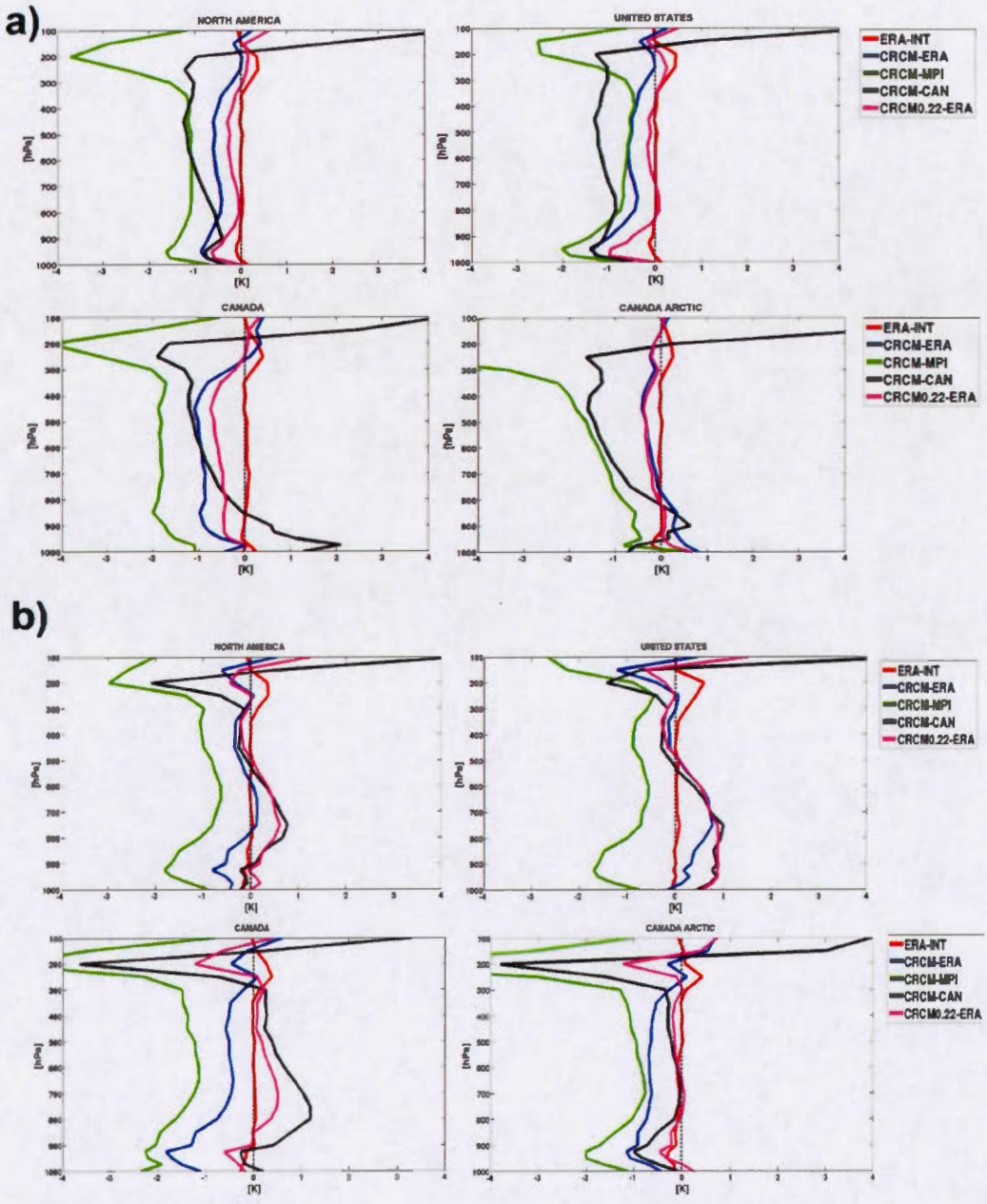

Figure 2.11 Vertical temperature profile bias averaged over North America and the three sub-domains (United States, Canada and Arctic) in: a) winter and b) summer season.

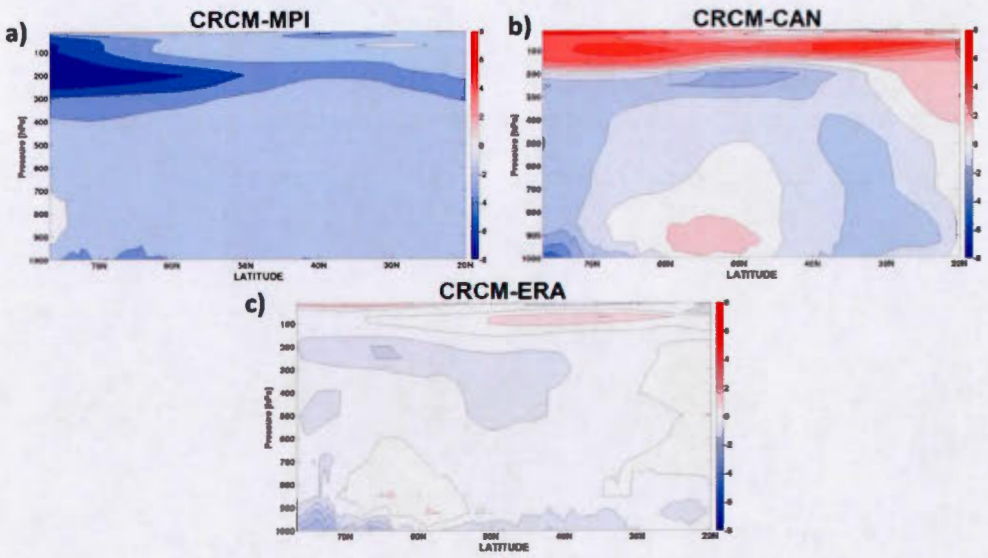

Figure 2.12 Mean zonal temperature differences from ERA-Interim for: a) CRCM-MPI, b) CRCM-CAN and c) CRCM-ERA.

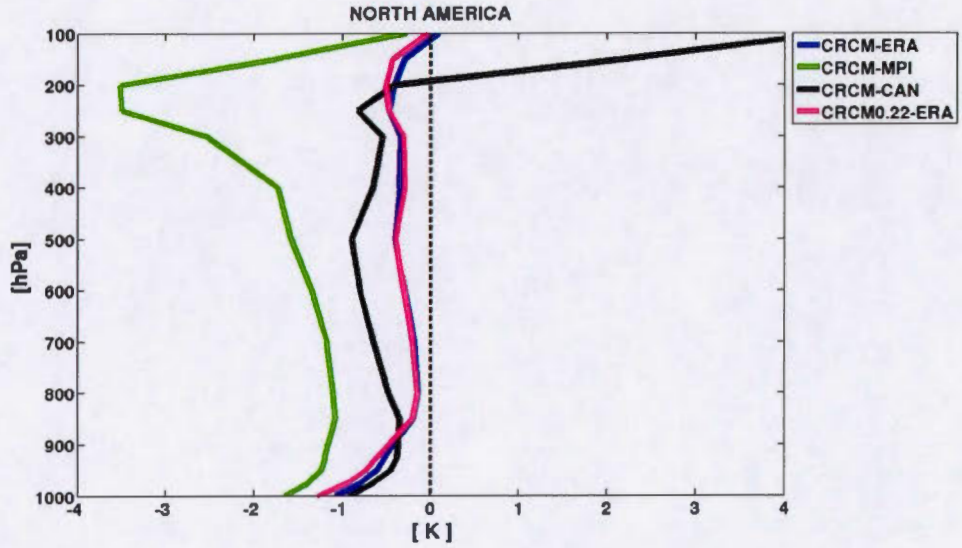

Figure 2.13 Vertical temperature profile mean bias against ERA-Interim over the whole North America in winter season.

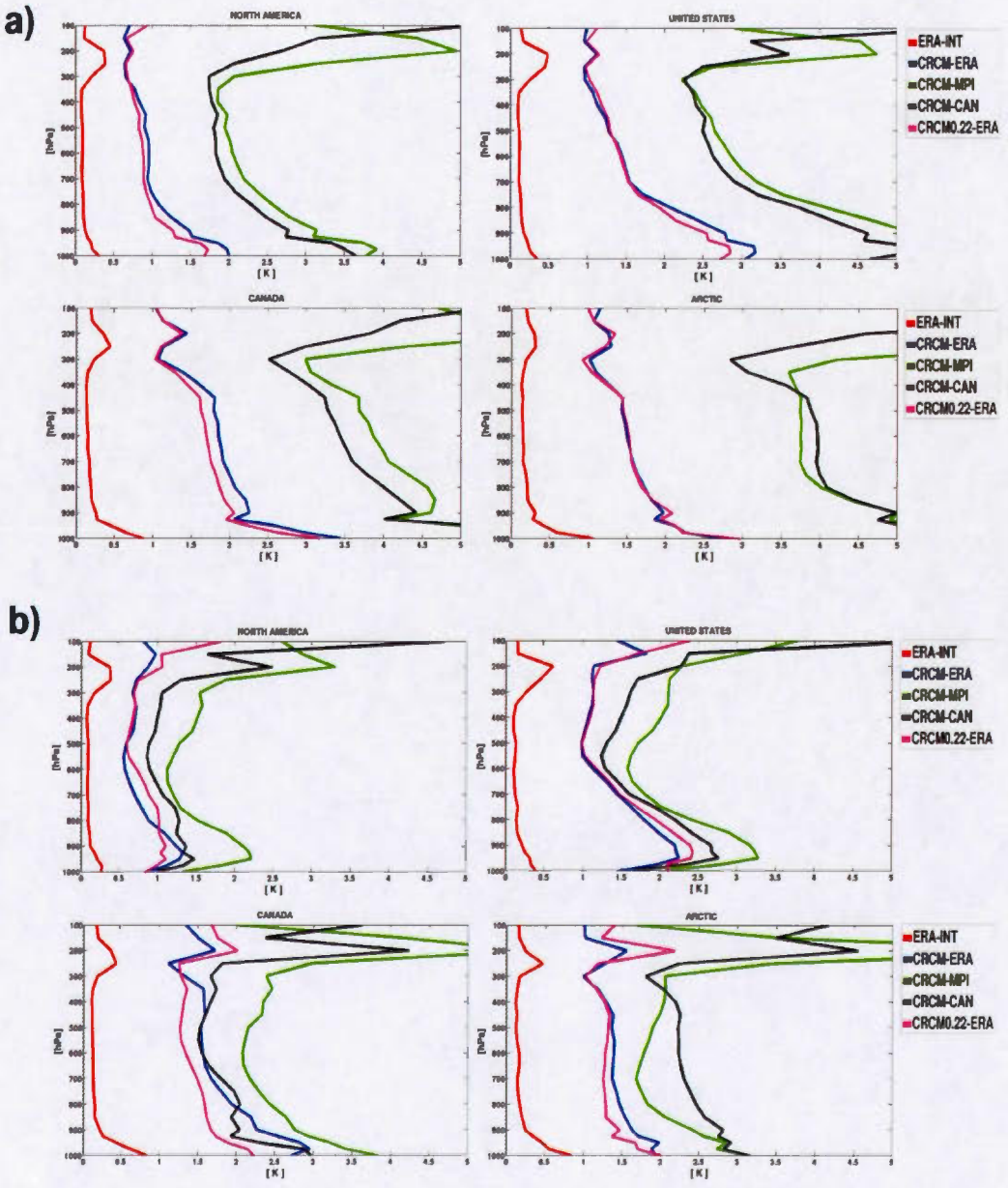

Figure 2.14 Vertical temperature profile root mean square error averaged over and the three sub-domains (United States, Canada and Arctic) in: a) winter and b) summer season.

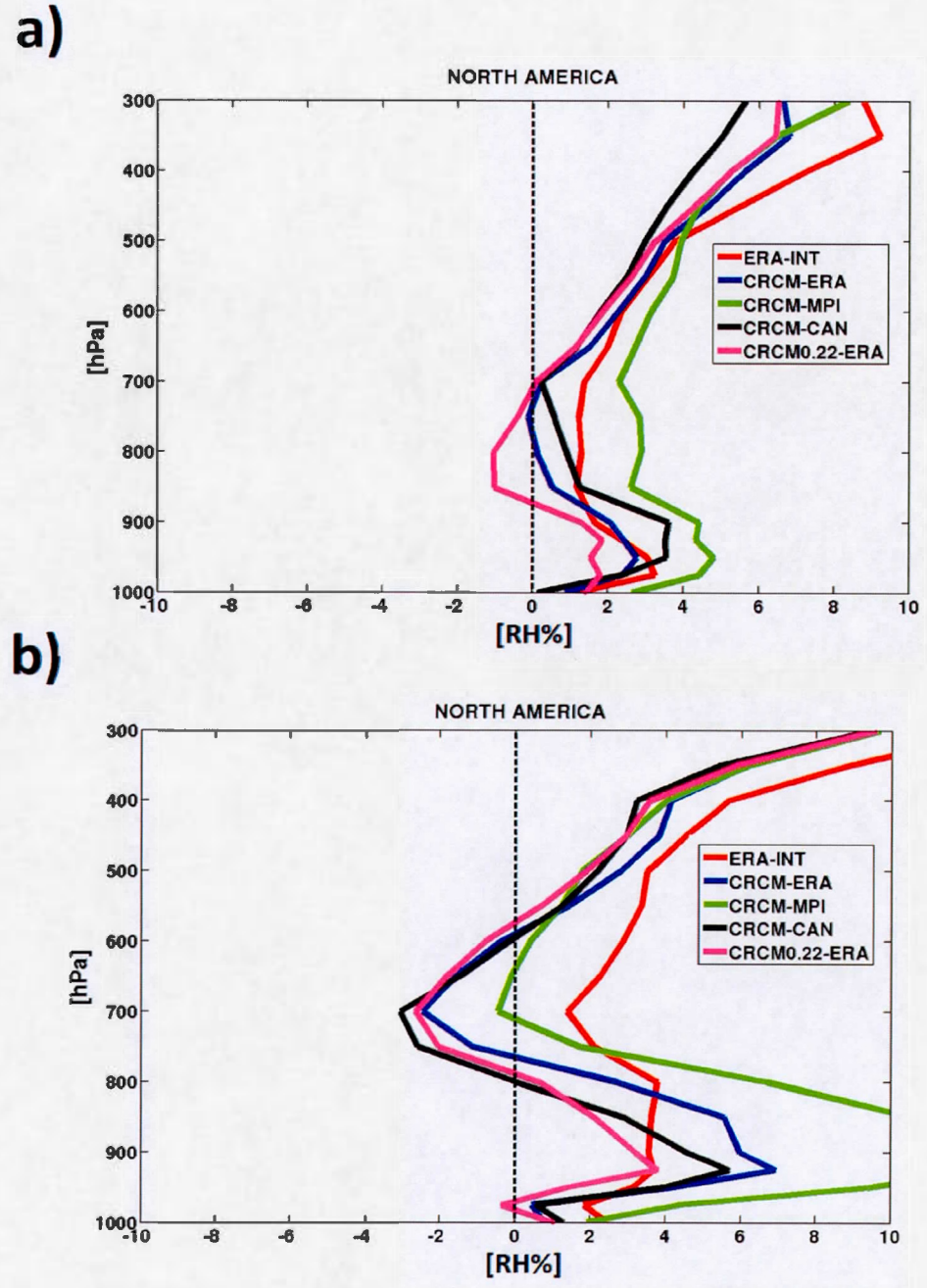

Figure 2.15 Vertical relative humidity profile bias averaged over North America in a) winter and b) summer season.

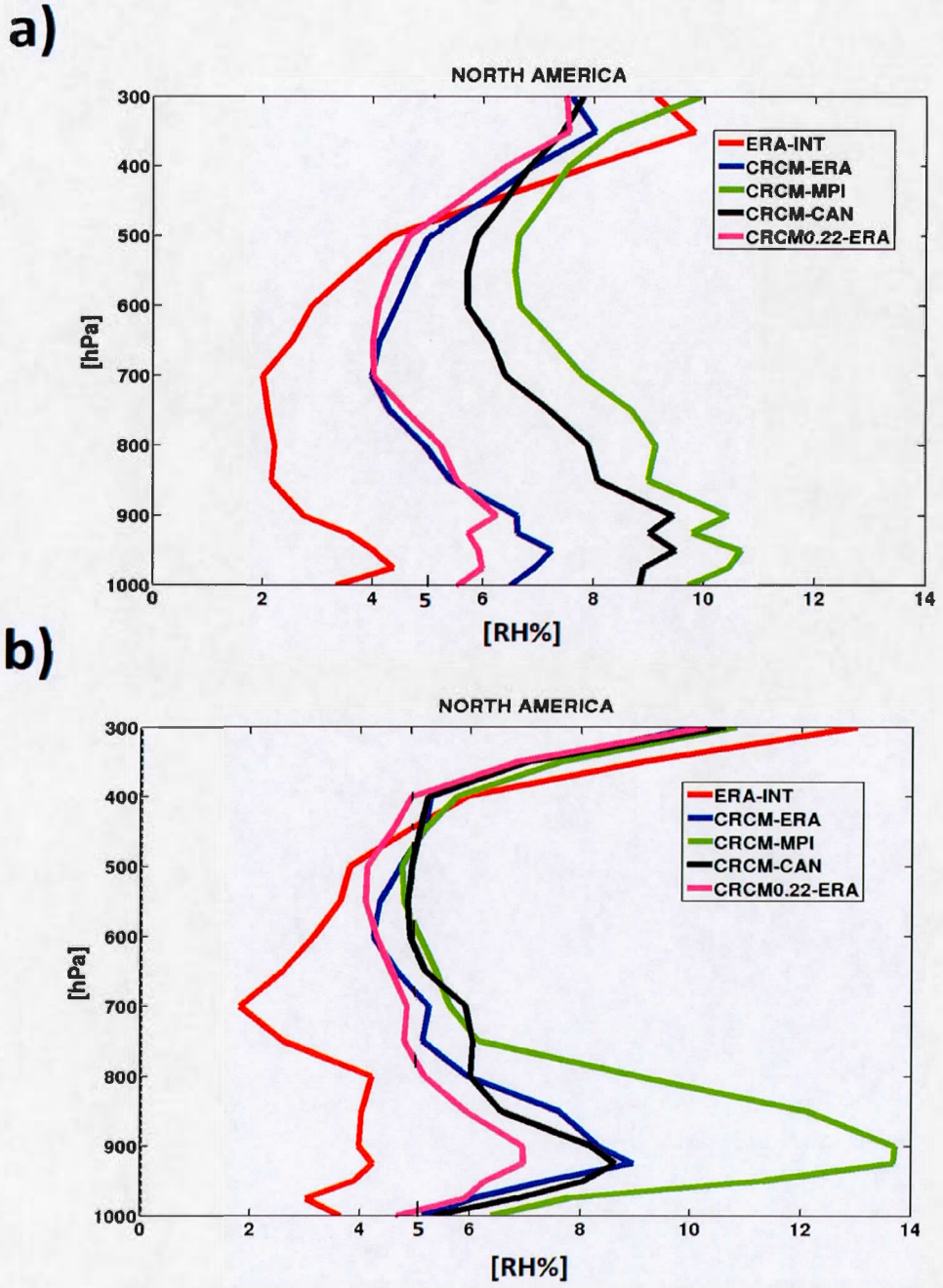

Figure 2.16 Vertical relative humidity profile root mean square error averaged over North America in: a) winter and b) summer season.

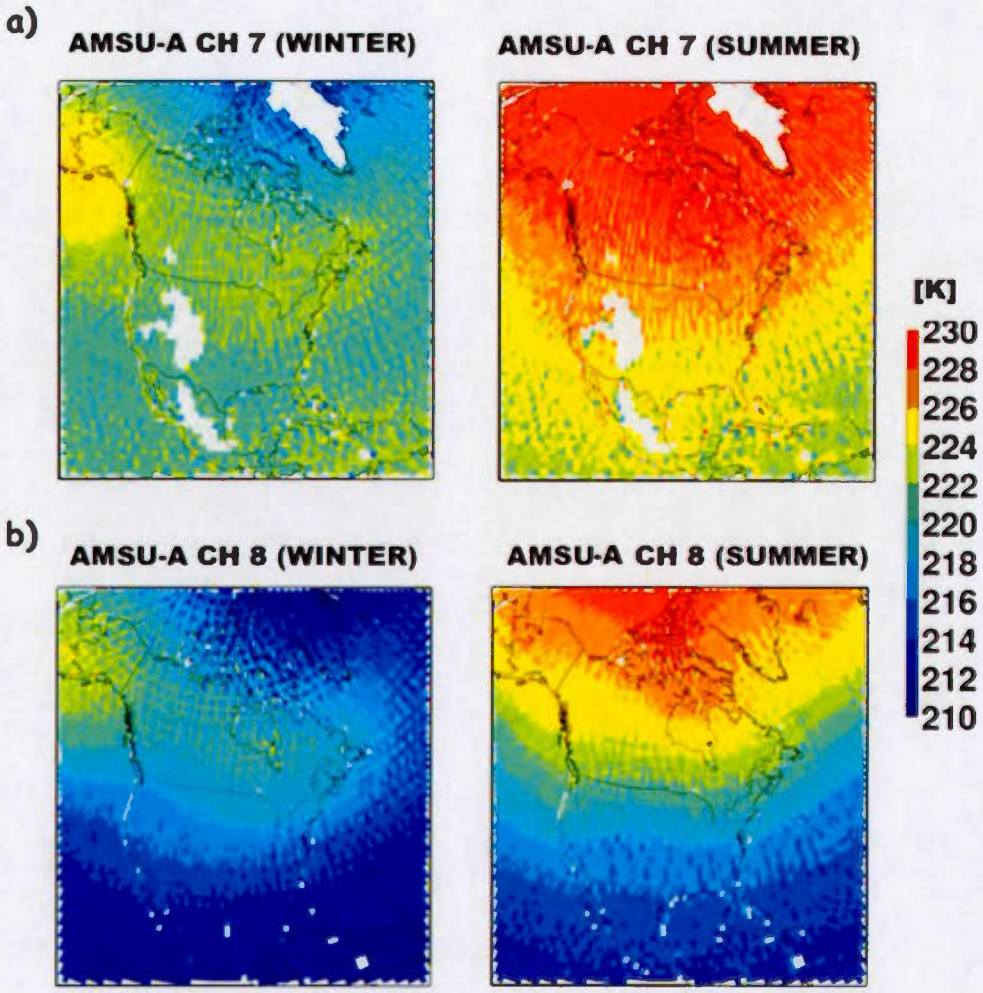

Figure 2.17 Spatial distribution of mean observed brightness temperature AMSU-A in winter (left) and summer (right) seasons for: a) Channel 7 and b) Channel 8.

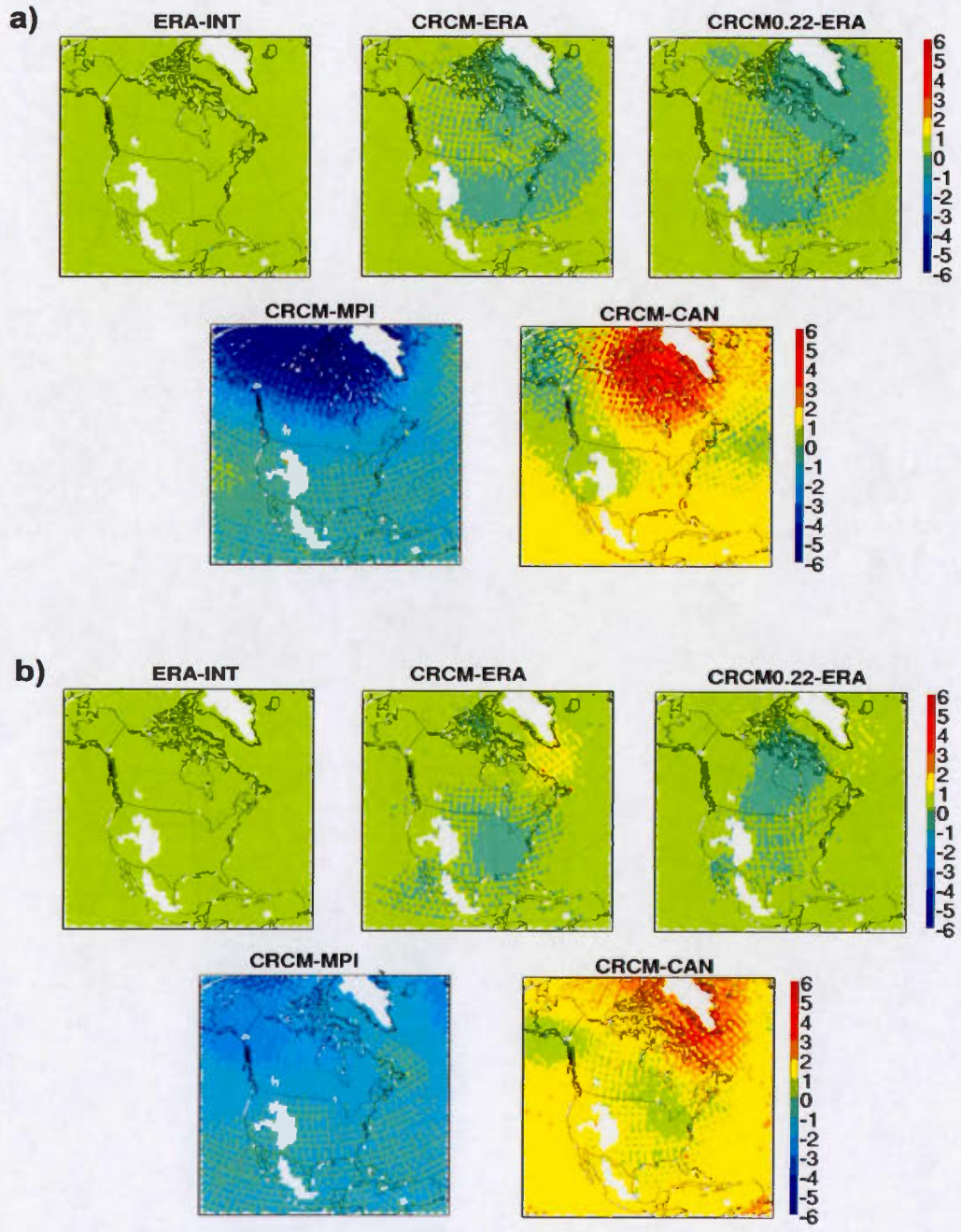

Figure 2.18 Spatial distribution of simulated brightness temperature mean bias with respect to AMSU-A Channel 7 observations in: a) winter and b) summer season.

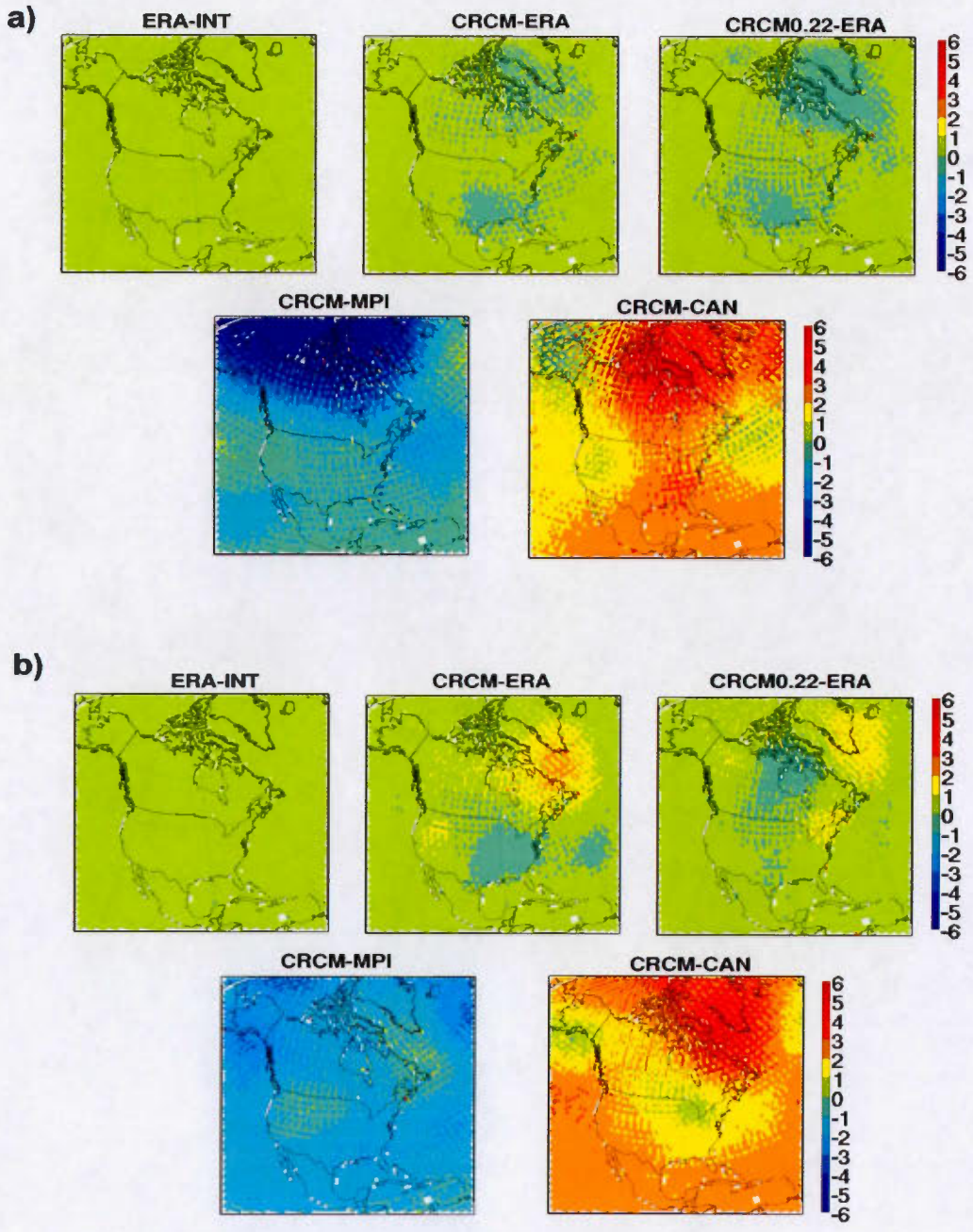

Figure 2.19 Same as in Fig 2.18 but for Channel 8.

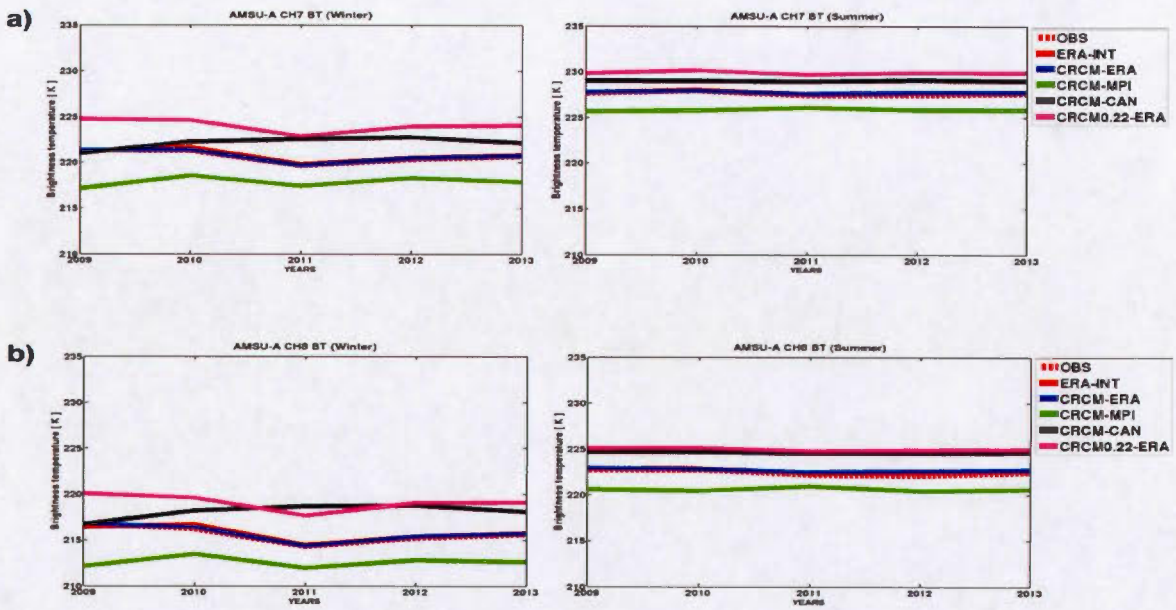

Figure 2.20 Mean annual observed and simulated brightness temperature evolution over North America in winter and summer seasons for AMSU-A: a) Channel 7 and b) Channel 8

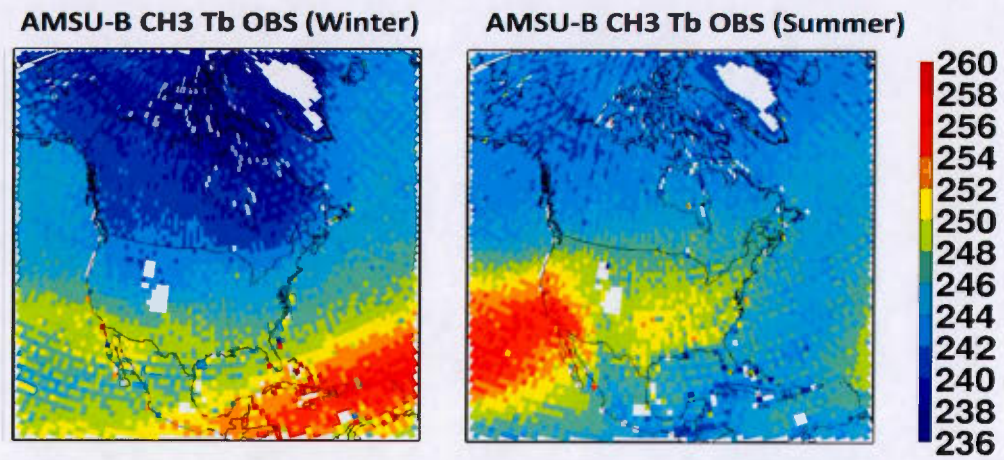

Figure 2.21 Spatial distribution of mean observed brightness temperature AMSU-B Channel 3 in winter (left) and summer (right) seasons.

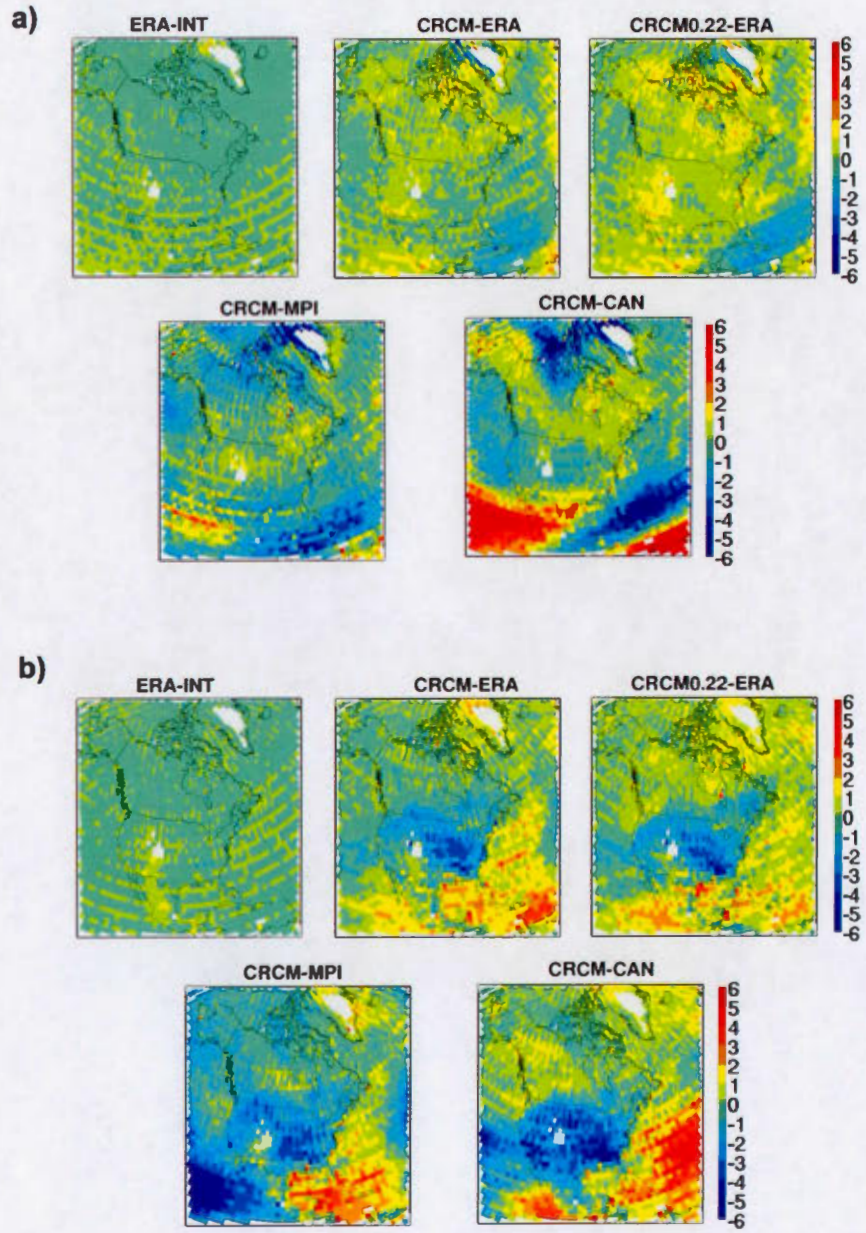

Figure 2.22 Spatial distributions of simulated brightness temperature mean bias with respect to AMSU-B Channel 3 observations in: a) winter and b) summer season

TABLEAUX

Observation Type	Data frequency	Reference variables
Surface weather stations (METARs, SYNOPs and SHIPs)	6 hours	2 m surface air temperature
Radiosondes	12 hours	Temperature, Relative humidity
Satellite radiances (AMSU-A Channel 7 and 8)	Time window of ±3 hours, every 6 hours	Brightness temperature sensitive to temperature
Satellite radiances (AMSU-B Channel 3)	Time window of ±3 hours, every 6 hours	Brightness temperature sensitive to water vapour

Table 2.1 Summary of observation type used and assessed variables

Simulation experiment	Horizontal resolution	Driving data	Reference publication
CRCM-ERA	0.44°	ERA-Interim reanalysis	Martynov et al, (2013)
CRCM0.22-ERA	0.22°	ERA-Interim reanalysis	Martynov et al, (2013)
CRCM-MPI	0.44°	Max Planck Institute for Meteorology's Earth System model	Separovic et al. (2013)
CRCM-CAN	0.44°	Second-Generation Canadian Earth system model	Separovic et al. (2013)
ERA-INT	0.75°	No driving data	Dee et al. (2011)

Table 2.2 Summary of the configurations of the climate simulations and reanalysis data used

RÉFÉRENCES

Athanasiadis P, Wallace J, Wettstein J (2010). Patterns of Wintertime Jet Stream Variability and Their Relation to the Storm Tracks. *Journal of the Atmospheric Sciences*, **67**, 1361–1381.

Bao X, Zhang F (2013). Evaluation of NCEP–CFSR, NCEP–NCAR, ERA-Interim, and ERA-40 Reanalysis Datasets against Independent Sounding Observations over the Tibetan Plateau. *Journal of Climate*, **26**, 206–214.

Buehler S.A., John V (2005). A simple method to relate microwave radiances to upper tropospheric humidity. Journal of Geophysical Research.

Buehler SA, Kuvatov M, John VO, Milz M, Soden BJ, Jackson DL, Notholt J (2008). An upper tropospheric humidity data set from operational satellite microwave data. Journal of Geophysical Research.

Chang E, Lee S, Swanson K (2002). Storm Track Dynamics. Journal of Climate 15:2163–2183.

Chouinard, C, Hallé, J (2003). Use of moisture sensitive satellite radiances in the Canadian Meteorological Centre Unified 3D-var system. Applications with Weather Satellites.

Dee D, Uppala (2009). Variational bias correction of satellite radiance data in the ERA-Interim reanalysis. Quarterly Journal of the Royal Meteorological Society 135:1830–1841.

Dee D, Uppala S, Simmons A, Berrisford, Poli, Kobayashi, Andrae, Balmaseda M, Balsamo, Bauer, Bechtold, Beljaars A, van de Berg, Bidlot, Bormann, Delsol (2011). The ERA-Interim reanalysis: configuration and performance of the data assimilation system. Quarterly Journal of the Royal Meteorological Society 137:553–597.

Deeter MN, Vivekanandan J (2005). AMSU-B Observations of Mixed-Phase Clouds over Land. Journal of Applied Meteorology 44:72–85.

Forster P, Andrews T, Good P, Gregory J, Jackson L, Zelinka M (2013). Evaluating adjusted forcing and model spread for historical and future scenarios in the CMIP5 generation of climate models. Journal of Geophysical Research: Atmospheres 118:1139–1150.

Gauthier P, Charrette C, Fillion L, Koclas P, Laroche S (1999). Implementation of a 3D variational data assimilation system at the Canadian Meteorological Centre. Part I: The global analysis. Atmosphere-Ocean 37:103–156.

Gauthier, P., C. Chouinard and B. Brasnett, 2003: Quality control: methodology and applications. In*Data Assimilation for the Earth System:* NATO Science Series. IV. Earth and Environmental Sciences, vol. 26, p.177-187.

Gauthier, P., M. Tanguay, S. Laroche S. Pellerin and J. Morneau, 2007: Extension of 3D-Var to 4D-Var: implementation of 4D-Var at the Meteorological Service of Canada. *Mon. Wea. Rev.*,**135**, 2339-2354.

Harris I, Jones PD, Osborn TJ, Lister DH (2013). Updated high-resolution grids of monthly climatic observations - the CRU TS3.10 Dataset. International Journal of Climatology 34:623–642.

Hernández-Díaz L, Laprise R, Sushama L, Martynov A, Winger K, Dugas B (2012). Climate simulation over CORDEX Africa domain using the fifth-generation Canadian Regional Climate Model (CRCM5). Climate Dynamics 40:1415–1433.

Hong S-Y, Kanamitsu M (2014). Dynamical downscaling: Fundamental issues from an NWP point of view and recommendations. Asia-Pacific Journal of Atmospheric Sciences 50:83–104.

Iacono, M.J. (2003). Evaluation of upper tropospheric water vapor in the NCAR Community Climate Model (CCM3) using modeled and observed HIRS radiances. Journal of Geophysical Research.

Iacono MJ, Mlawer EJ, Clough SA, Morcrette J-J (2000). Impact of an improved longwave radiation model, RRTM, on the energy budget and thermodynamic properties of the NCAR community climate model, CCM3. Journal of Geophysical Research 105:14873.

Jakobson E, Vihma T, Palo T, Jakobson L, Keernik H, Jaagus J (2012) Validation of atmospheric reanalyses over the central arctic ocean. Geophysical Research Letters 39.

John V, Soden B (2007). Temperature and humidity biases in global climate models and their impact on climate feedbacks. Geophysical Research Letters.

Jolliffe IT, Stephenson PDB (2012). Forecast Verification: A Practitioner's Guide in Atmospheric Science, 2nd Edition. Wiley, United Kingdom

Kabela ED, Carbone GJ (2015). NARCCAP Model Skill and Bias for the Southeast United States. American Journal of Climate Change 04:94–114.

Kidder SQ, Goldberg MD, Zehr RM, DeMaria M, Purdom JFW, Velden CS, Grody NC, Kusselson SJ (2000). Satellite Analysis of Tropical Cyclones Using the Advanced Microwave Sounding Unit (AMSU). Bulletin of the American Meteorological Society 81:1241–1259.

Martynov, Laprise, Sushama, Winger, Šeparović, Dugas (2013). Reanalysis-driven climate simulation over CORDEX North America domain using the Canadian Regional Climate Model, version 5: model performance evaluation. Climate Dynamics 41:2973–3005.

Mearns LO, Arritt R, Biner S, Bukovsky MS, McGinnis S, Sain S, Caya D, Correia J, Flory D, Gutowski W, Takle ES, Jones R, Leung R, Moufouma-Okia W, McDaniel L, Nunes AMB, Qian Y, Roads J, Sloan L, Snyder M (2012). The North American Regional Climate Change Assessment Program: Overview of Phase I Results. Bulletin of the American Meteorological Society 93:1337–1362.

Miloshevich L, Vömel H, Paukkunen A, Heymsfield A, Oltmans S (2001). Characterization and Correction of Relative Humidity Measurements from Vaisala RS80-A Radiosondes at Cold Temperatures. Journal of Atmospheric and Oceanic Technology 18:135–156.

Milz M, Buehler SA, John VO (2009). Comparison of AIRS and AMSU-B monthly mean estimates of upper tropospheric humidity. Geophysical Research Letters.

Mooney P, Mulligan F, Fealy (2011). Comparison of ERA-40, ERA-Interim and NCEP/NCAR reanalysis data with observed surface air temperatures over Ireland. International Journal of Climatology 31:545–557.

Paltridge G, Arking A, Pook M (2009). Trends in middle- and upper-level tropospheric humidity from NCEP reanalysis data. Theoretical and Applied Climatology 98:351–359.

Pierce DW, Barnett TP, Santer BD, Gleckler PJ (2009). Selecting global climate models for regional climate change studies. Proceedings of the National Academy of Sciences 106:8441–8446.

Rabier F, Järvinen H, Klinker E, Mahfouf J-F, Simmons A (2000). The ECMWF operational implementation of four-dimensional variational assimilation. I: Experimental results with simplified physics. Quarterly Journal of the Royal Meteorological Society 126:1143–1170.

Reynolds R, Rayner N, Smith T, Stokes D, Wang W (2002). An Improved In Situ and Satellite SST Analysis for Climate. Journal of Climate 15:1609–1625.

Rosenkranz PW (2001). Retrieval of temperature and moisture profiles from AMSU-A and AMSU-B measurements. IEEE Transactions on Geoscience and Remote Sensing 39:2429–2435.

Sapucci L, Machado L, da Silveira R, Fisch G, Monico J (2005). Analysis of Relative Humidity Sensors at the WMO Radiosonde Intercomparison Experiment in Brazil. Journal of Atmospheric and Oceanic Technology 22:664–678. Saunders RW, Hewison TJ, Stringer SJ, Atkinson NC (1995). The radiometric characterization of AMSU-B. IEEE Transactions on Microwave Theory and Techniques 43:760–771.

Saunders R, Matricardi M, Brunel P (1999). An improved fast radiative transfer model for assimilation of satellite radiance observations. Quarterly Journal of the Royal Meteorological Society 125:1407–1425.

Schmidt G, Ruedy R, Miller R, Lacis A (2010). Attribution of the present-day total greenhouse effect. Journal of Geophysical Research.

Scinocca J, McFarlane N, Lazare, Li, Plummer (2008). Technical Note: The CCCma third generation AGCM and its extension into the middle atmosphere. Atmospheric Chemistry and Physics 8:7055–7074.

Šeparović L, Alexandru A, Laprise R, Martynov A, Sushama L, Winger K, Tete K, Valin M (2013). Present climate and climate change over North America as simulated by the fifth-generation Canadian regional climate model. Climate Dynamics 41:3167–3201.

Simmons A (2004). Comparison of trends and low-frequency variability in CRU, ERA-40, and NCEP/NCAR analyses of surface air temperature. Journal of Geophysical Research.

Simmons A, Poli P, Dee D, Berrisford P, Hersbach H, Kobayashi S, Peubey C (2014). Estimating low-frequency variability and trends in atmospheric temperature using ERA-Interim. Quarterly Journal of the Royal Meteorological Society 140:329–353.

Simmons A, Poli P (2014). Arctic warming in ERA-Interim and other analyses. Quarterly Journal of the Royal Meteorological Society.

Stevens B, Giorgetta M, Esch M, Mauritsen T, Crueger T, Rast S, Salzmann M, Schmidt H, Bader J, Block K, Brokopf R, Fast I, Kinne S, Kornblueh L, Lohmann

U, Pincus R, Reichler T, Roeckner E (2013). Atmospheric component of the MPI-M Earth System Model: ECHAM6. Journal of Advances in Modeling Earth Systems 5:146–172.

Trenberth KE, Guillemot CJ (1998). Evaluation of the atmospheric moisture and hydrological cycle in the NCEP/NCAR reanalyses. Climate Dynamics 14:213–231.

Villarini G, Vecchi G (2013). Projected Increases in North Atlantic Tropical Cyclone Intensity from CMIP5 Models. Journal of Climate 26:3231–3240.

Willmott CJ, Matsuura K (1995). Smart Interpolation of Annually Averaged Air Temperature in the United States. Journal of Applied Meteorology 34:2577–2586.

Willmott CJ, Robeson SM (1995). Climatologically aided interpolation (CAI) of terrestrial air temperature. International Journal of Climatology 15:221–229.